DESIGN AND ANALYSIS OF CAPACITIVELY-FED FOLDED SLOT AND RECTANGULAR PATCH ANTENNA FOR BODY CENTRIC WIRELESS COMUNICATIONS

By:

Emmanuel Valentín-Hernández

A Thesis Submitted in Partial Fulfillment of the Requirements for the Degree of:

MASTER OF SCIENCE

In

Electrical Engineering

UNIVERSITY OF PUERTO RICO
MAYAGUEZ CAMPUS

May 2015,

Approved By:

_____	_____
José G. Colom-Ustariz, Ph.D Member, Graduate Committee	Date
_____	_____
Dejan S. Filipovic, Ph.D Member, Graduate Committee	Date
_____	_____
Eduardo J. Juan-García, Ph.D Member, Graduate Committee	Date
_____	_____
Rafael Rodríguez Solís, Ph.D President, Graduate Committee	Date
_____	_____
Silvina Cancelos, Ph.D Representative of Graduate Studies	Date
_____	_____
Raúl E. Torres Muñiz, Ph.D Director, Electrical and Computer Engineer Department	Date

Abstract of Dissertation Presented to the Graduate School
Of the University of Puerto Rico in Partial Fulfillment of the
Requirements for the Degree of Master of Science

DESIGN AND ANALYSIS OF CAPACITIVELY-FED FOLDED SLOT AND RECTANGULAR PATCH ANTENNA FOR BODY CENTRIC WIRELESS COMUNICATIONS

By
Emmanuel Valentín Hernández

May 2015

Chair: Rafael A. Rodríguez Solís
Major Department: Electrical and Computer Engineering

In this thesis two antenna configurations are designed and modified, to operate in the 2.45 GHz ISM Band, to be used in body centric wireless communication applications. The two configurations were a Capacitively-Fed Folded Slot Antenna and a Rectangular Patch Antenna. The rectangular patch was modified to work as a quarter wavelength structure with three loading slots, and by adding a parasitic patch. This new modified configuration represents a contribution for this work. After the modifications, a bandwidth of 100 MHz and gain of 4.5dB were achieved. The capacitively-fed folded slot antenna was modified by adding eight loading slots which represents another contribution of this work. With this modification the antenna length was reduced to 16 mm in a 40 mm by 40 mm ground plane with a gain of 4.27 dB, and bandwidth of 20 MHz. Both antennas were fabricated and measured in the UPRM Microwave and Millimeter-Wave System Laboratory to validate the results obtained from simulations

The effect of the human body was analyzed by simulations with a uniform model of the human body developed during the research. The human body does not show a significant effect in antenna performance. This effect was seen in both of the proposed antennas.

Resumen de Tesis Presentado a Escuela Graduada
De la Universidad de Puerto Rico como requisito parcial de los
Requerimientos para el grado de Maestría en Ciencias

DISEÑO Y ANÁLISIS DE UNA ANTENA DE RANURA PLEGADA ALIMENTADA POR ACOPLE CAPACITIVO Y UNA ANTENA DE PARCHO RECTANGULAR PARA LA APLICACIÓN DE COMUNICACIÓN INALÁMBRICA CENTRADA EN EL CUERPO

Por

Emmanuel Valentín Hernández

Mayo 2015

Consejero: Rafael A. Rodríguez Solís
Departamento: Ingeniería Eléctrica y de Computadoras

En esta tesis una antena de ranura plegada alimentada por acople capacitivo y una antena de parche rectangular, son diseñadas y modificadas, con el fin de ser utilizadas para aplicaciones de comunicaciones inalámbricas centradas en el cuerpo en la banda ISM de 2.45 GHz. El parche rectangular fue modificado para operar como una estructura de un cuarto de largo de onda con tres ranuras de carga, y añadiendo un parche parasítico, lo que representa una de las contribuciones de este trabajo. Con las modificaciones se logró cumplir con un ancho de banda de 100 MHz, y una ganancia de 4.5 dB. En el caso de la antena de ranura plegada, se modificó añadiendo ocho ranuras de carga, lo que representa la segunda contribución de este trabajo. La modificación realizada a esta antena logró reducir su largo a 16 mm en un plano de tierra de 40 mm por 40 mm con un ancho de banda de 20 MHz y una ganancia de 4.27 dB.

El efecto del cuerpo humano fue estudiado mediante simulaciones utilizando un modelo uniforme del cuerpo humano desarrollado durante la investigación. El cuerpo humano reflejo un efecto no significativo en el comportamiento de la antena. Dicho efecto se observó en las dos antenas.

To the memory of my loved godmother

ACKNOWLEDGEMENS

First, thanks to God to give me the health, wisdom, and all of the necessary tools to complete this goal in my live. Thanks to my parents, my sister and Jessenia for their support, love, and comprehension during this time and for serving me as an inspiration to keep going. To my two angels, Dr. Madeline J. Rodríguez and Sandra Montalvo, thanks for always advising me to keep me focused and on the right way no matter the circumstances. I also want to express my gratitude to Dr. Jose G. Colom Ustáriz and Dr. Eduardo J. Juan as members of my graduate committee. Special thanks to Dr. Dejan S. Filipovic, for his advisement and teachings during the summer 2014. Thanks for giving me the opportunity of work with you, for teaching me more about this awesome world of antenna engineering, and also for the honor to have you as a member of my graduate committee.

Finally, thanks to my advisor Dr. Rafael Rodríguez Solís. I have no words to express my gratitude to him. Thanks for believing in me and for giving me this awesome experience. Thanks for showing and teaching me the amazing word of the electromagnetics, for always being accessible to clarify doubts no matter if we were in the classroom, in the office, or the hallway.

Table of Contents

Page

List of Tables

Table **Page**

List of Figures

Page

CHAPTER 1
INTRODUCTION

Over the past few years, an increased interest in Body Centric Wireless Communications has made this research field very popular in terms of the theoretical studies and the development of many devices and systems for different applications [1]. One of these applications is focused in the protection of people in different scenarios using sensors to monitor vital signs, for example patients in hospitals, soldiers in the battlefield, and first responses in emergency situations [2]. With the development of medical devices and systems used on or in the human body, the wireless body area networks for sensing and monitoring the vital signs has received more and more attention, and are becoming one of the most rapid growing wireless communication systems [3]. For example, the U.S. Department of Defense is working on wireless devices to be worn by soldiers that will allow medics to measure vital signs and collect other medical information from the troops [4]. For this reasons, body-centric wireless communication systems (BWCS) will be a focal point for future communications from an end-to-end user's perspective [5].

Given that the person carrying the network will like to stay comfortable and maintain ease of movement, the antennas should be low profile, compact in size, and low cost for convenience in use [3]. Thus compact, small size and better performance antennas are required to operate in such systems [6]. Because the application requires that the antennas should be placed on or near the body, the antennas should to have a unidirectional radiation pattern to reduce the interaction between the human body and the antennas. Therefore, it is very important to correctly model the electrical properties of the human body to properly design the antennas, in terms of input impedance and radiation pattern, and reduce the energy absorbed by the body.

1.1 Objectives

The main goal of this project is to design an antenna for Body Centric Wireless Communication (BCWC) applications. The antenna is designed to operate in the 2.45 GHz ISM Band with 85 MHz of Bandwidth and a unidirectional radiation pattern to avoid the radiation of the antenna to the human body. An analysis of the antenna performance with the human body is also desired for this work. With this analysis, the antenna will have a good performance when placed on the human body.

Previous works in BCWC in the ISM bands show antennas using multilayer structures or air as a substrate to achieve with the desired bandwidth. As a contribution, this work presents two new modified antenna configurations designed as a single layer structure with a solid rigid substrate, to provide a more rugged construction for this application.

1.2 Work Organization

The background and previous work in Body-Centric Wireless Communication, modeling of the human body, antenna miniaturization techniques, and a brief description and background of Design of Experiments, will be presented in Chapter 2. Chapter 3 presents all of the methodology used to complete this work. The design of the different types of the antennas and the modeling of the human body are presented in this chapter. Chapter 4 presents the results and discussion of the designed antenna configurations and their validation. The results of the human body model also are presented in this chapter. Chapter 5 will present the conclusions and recommendations for future work about this research.

CHAPTER 2
LITERATURE REVIEW AND BACKGROUND

The work in antennas for body-centric wireless communications can be divided into two areas: (i) the design and modeling of the antenna, (ii) and the modeling of the human body. However, the design of the antenna cannot be separated from the human body environment. It sets out requirements on the design parameters of the antenna. For the antenna, some of these requirements are: Low profile, small size, low power and unidirectional radiation pattern. For the human body, a good model should be used to consider the interaction with the antenna performance. It should consider the electromagnetic properties at the operational frequency, and the position of the human body, as well the position of the antenna. This chapter will present a background in Body-Centric Wireless Communications. Also a brief description and background of Design of Experiment will be discussed as a characterization method.

2.1 Modeling of the Human Body

Human body models can vary in complexity. You can have simple computational models to model the tissues in layers, or use detailed models of the body that would allow studying not only the effect of the tissues, but also the effect of the antenna position on the body and the body position. Software like Remcom's XFDTD provide a human body model in which the antenna can be placed, but requires a large computational time to make the mesh and complete the simulations. It may take hours or days, depending on the mesh resolution. Simplified computational models of the human body that allows the study in BCWC are presented in the literature.

Guangdong, et. al. [3], used a multilayer cube that considered the electromagnetic properties of the skin, muscle and fat at 2.45GHz. Chia-Hsien, et. al. [4], modeled the human body in three different ways; a multi-layered structure, a homogeneous cylinder, and six-side structures, also with the electromagnetics properties of the human body at 2.45GHz. Fig 2.1 to Fig 2.4 show the models described above. The electromagnetic properties of the human body used in these models can be obtained from P.Hall and Y.Hao [5].

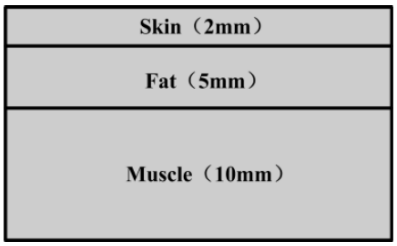

Figure 2.1: Three-Layer Model of the Human Body (*taken from [5]*)

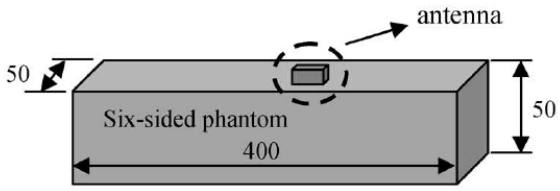

Figure 2.2: Six-Side Model of the Human Body (taken from [7])

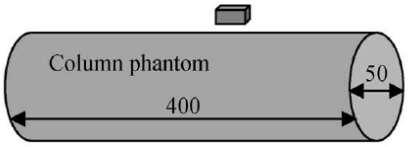

Figure 2.3: Column Model of the Human Body (taken from [7])

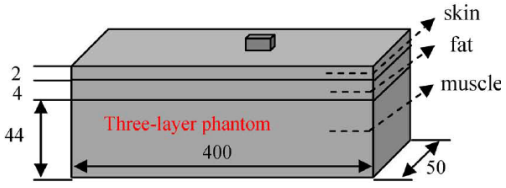

Figure 2.4: Three-Layer Model of the Human Body (taken from [7])

A way of physically modeling the human tissues is by the use of phantoms. A phantom can be defined as a biological body or as physical model simulating the characteristics of the

biological tissues [5]. Although the human body can be thought of comprised by layers, each of them with specific electromagnetic properties, the phantoms are created as homogenous structures due to the complexity of fabricating a layered structure. Phantoms can be classified as liquid, semi-solid, and solid [1]. Liquid phantoms consist of a container, with the shape of the body part, filled with a liquid with the desired electromagnetic properties. Semi-Solid phantoms consist of a liquid with a coagulant agent added to create a gel with the desired electromagnetic properties. Solid phantoms have been proposed at frequencies up to 6 GHz, based on various materials [1]. This type of phantom has longer lifespan, and require a complex process to fabricate it.

Figure 2.5 Solid Phantom of Carbon-loaded silicon rubber [1]

2.2 Antennas for Body Centric Wireless Communication

A simple antenna configuration used for BCWC is the microstrip patch antenna. Guangdong, et. al. presented a dual band shorted patch which works at 2.45 GHz and 5.8 GHz in [3]. This structure has many advantages as low radiation loss, low dissipation, and easy to integrate with RF or microwave circuit component, to perform a miniature hybrid or monolithic microwave integrated circuit. The configuration consists of a rectangular patch with two shorting

pins in the bottom edges to make the patch a quarter wave structure. The patch also has a U-slot, which makes the antenna dual-band. The patch size is 22 mm x 16 mm with a bandwidth of 4% for 2.45GHz and 3.5% for 5.8 GHz in a substrate with a dielectric constant of 4.4 and thickness of 1.6 mm. Fig 2.6 shows the antenna configuration.

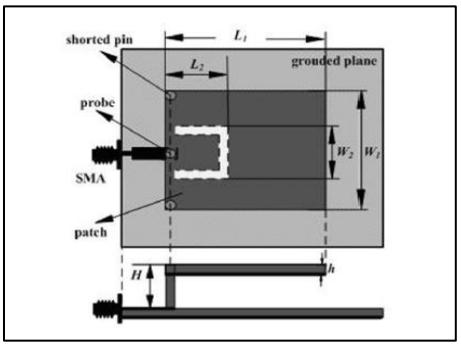

Figure 2.6 Antenna Configuration taken from [3]

Chadran, et. al., presents another work with a microstrip patch antenna in [8]. In this work, a microstrip patch antenna at 2.45 GHz is designed to have a switching pattern to use for off-body and on-body systems. The patch was designed to be of 17 mm x 17 mm and is mounted in a substrate, close to the air (ε_r close to one), of 5.75 mm of height. The ground plane of the antenna is 50 mm by 50 mm. The patch is fed by a microstrip line placed in the ground plane, with a connecting post from the line to the patch. The antenna was modeled on a muscle phantom and provided an impedance bandwidth over the 200 MHz for each mode, and an efficiency of 57% was achieved in both cases. Fig 2.7 shows the antenna geometry and Fig 2.8 shows the results in return loss.

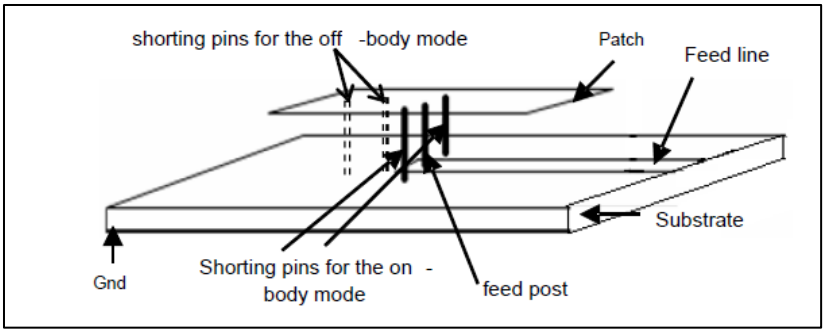

Figure 2.7 Cross-sectional view of the geometry presented in [8]

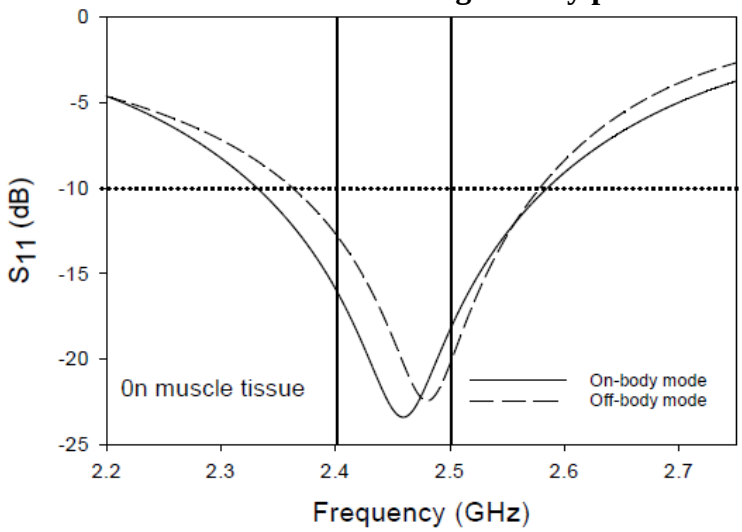

Figure 2.8 Comparison of on-body and off-body mode presented in [8]

A compact planar inverted-F antenna (PIFA) operating at 2.45 GHz is presented by Chia-Hsien, et. al. in [7]. Two shorting structures and a folded ground plane are used to improve the impedance matching and decrease the size of the proposed antenna [7]. The antenna geometry is a rectangular patch with a shorting pin and shorting plate, and is 26 mm x 26 mm x 4 mm of size with a ground plane of size 32 mm by 32 mm. The shorting pins and plate were used to improve the impedance matching. The antenna covered the 2.45 GHz ISM band and used the human body models shown in Fig 2.2 to Fig 2.4 to study the interaction between the antenna and the human body. Fig 2.9 and Fig 2.10 show the geometry of the antenna, and the gain pattern comparison between free space and human body placement, respectively.

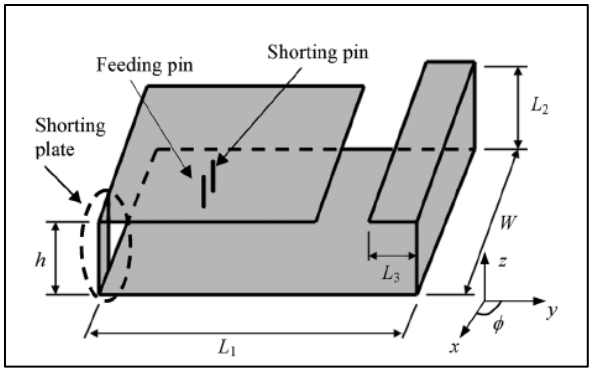

Figure 2.9: Planar Inverted F Antenna Presented in [7]

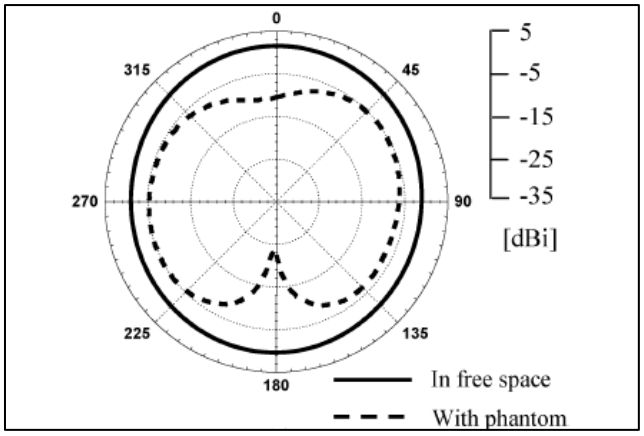

Figure 2.10 Radiation Pattern Comparison of [7]

Another two configurations used for BCWC are the Compact Ring Monopole Antenna presented in [6] and the Microstrip Fed Ground Modified Compact Antenna presented in [9]. Ramli, et. al. [6], provide a better understanding of antenna size reduction by adding stub and ground pin on small printed monopole antenna for narrowband applications [6]. In this paper the antenna is a ring shape monopole with a stub and a ground pin to adjust the impedance matching and tune the frequency, and it is designed to work from 2.4 GHz to 2.9 GHz. In this case the antenna works in an in-body application, as an implantable antenna, and it is modeled with a uniform layer model of the human body, as shown in Fig 2.11.

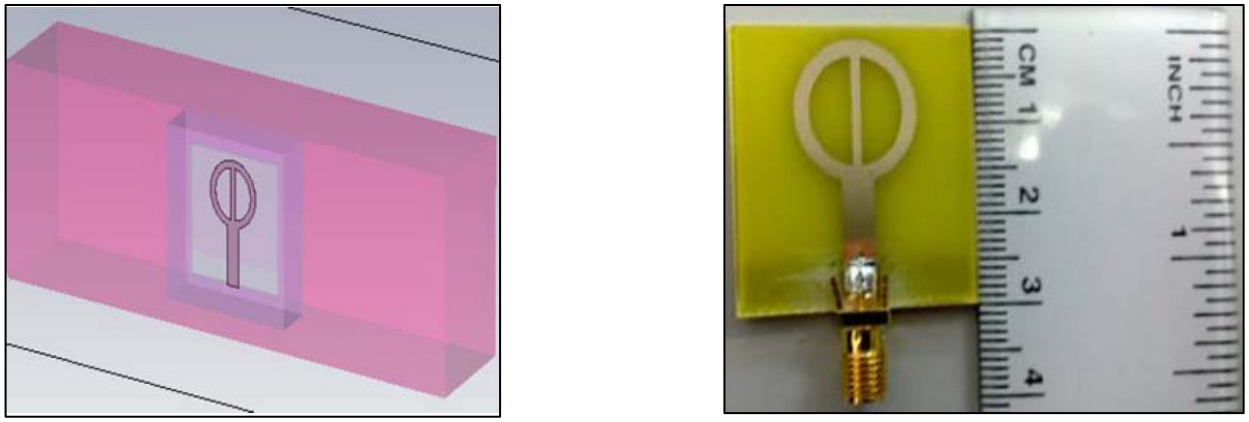

(a) (b)

Figure 2.11 (a) Model of the Human Body (Solid Pink Rectangle) with the Antenna (b) Antenna Geometry Presented in [6]

The configuration presented by Raman, et. al. consists in a compact truncated microstrip-fed ground meandered single band antenna with reconfigurable directional pattern [9]. The antenna has two switches to obtain different states of the radiation pattern and resonant frequency to make the antenna suitable for the BCWC applications. The overall dimensions of the antenna are 0.093λg x 0.23λg x 0.018λg, where λg is the guided wavelength corresponding to the resonant frequency [9].

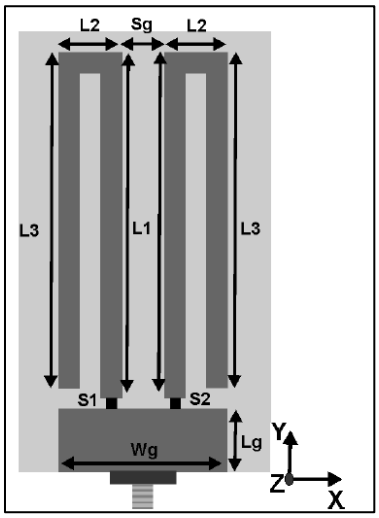

Figure 2.12 Geometry of the Antenna Presented in [9]

As shown in this section the antennas presented so far in the literature use air as substrate or a multilayer structured to meet with required bandwidth of the ISM band. For these reasons, and to obtain a rugged antenna, this work is intended to obtain an antenna in a single layer structure and using a rigid, solid substrate.

2.3 Antenna Miniaturization

As mentioned by Volakis, et. al. in [10], antenna miniaturization has long been discussed as one of the most significant and interesting subjects in antenna related fields. Small antennas, or electrically small antennas, as are defined in [10], are antennas with a size less than the half wavelength at resonant frequency. In [11], a 2.45 GHz electrically small slot antenna of $\frac{\lambda_0}{35} * \frac{\lambda_0}{35}$ was achieved through symmetric inductive loading of an electrically small slot as shown in Fig. 2.13. Another miniaturization technique is to use a shorted pin in the center of a patch in order to use the patch as a quarter wavelength structure as has been used in [3]. The addition of loading slots is also a miniaturization technique, due to the increase in the electrical length despite the reduction in the physical length.

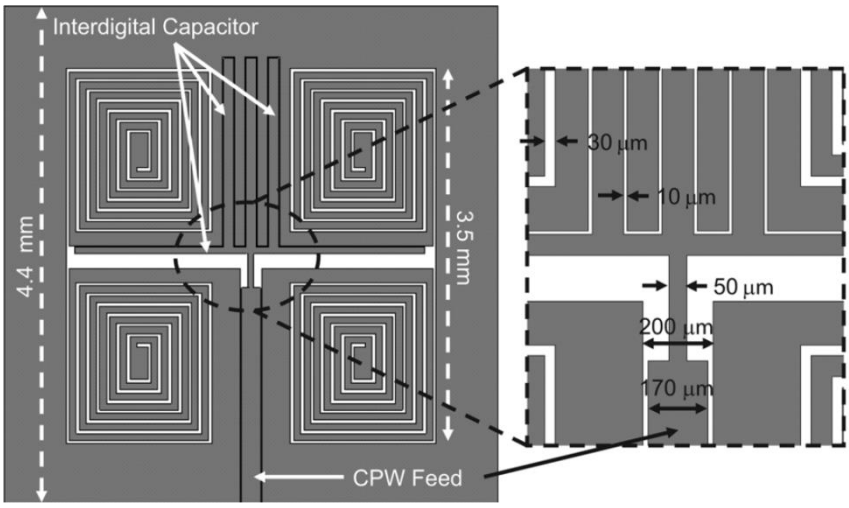

Figure 2.13: Electrically Small Slot Antenna in [11]

Wheeler discussed the fundamental limitations of small antennas using a simple model that approximates the antenna with a lumped capacitance or inductance and a radiation resistance [10]. Wheeler used the ratio between radiated power to reactive power (RPF) and concluded that the RPF was directly proportional to the antenna volume, which imposes a fundamental limit in bandwidth [10]. It can be shown with the Wheeler circuit model that the RPF is the inverse of the Q factor. Volakis also discussed the bending and folding as a miniaturization technique. This technique is due by folding the antenna structure in order to maintain the electrical length of the structure while the physical space is reduced.

2.4 *Slot Antennas*

This antenna type comprises a slot in the ground plane of a grounded substrate, and can have virtually any shape [12]. Folded-slots and circular slot-rings, among others, are some of the shapes that a slot antenna could have. Slot antennas are low profile, easy to fabricate, low cost and the matching network can be fabricated with the structure of the antenna. Another advantage of these antennas is the availability to produce bidirectional and unidirectional radiation pattern. Despite its advantages they suffer from undesired modes such as the parallel plate modes excited between the ground planes [12].

2.4.1 Folded Slot Antennas

Folded-slot antennas (FSAs) offer some of the attractive characteristics of the slot antennas, such as small size, light weight, wider bandwidth and that can be flush-mounted on surfaces, they also present an input impedance about four times lower than the slot antenna at the first useful resonance (f_0) which facilitate the matching to 50 Ω and providing a wider bandwidth [13]. The folded slot antenna can be fed by coplanar-waveguide (CPW), which has the

advantages of having all the conductors on the same substrate side, avoiding the use of vias through the substrate. The CPW feed could be inductive or capacitive as shown in Fig. 2.14.

a) Capacitive Feed b) Inductive Feed

Figure 2.14: CPW-Feed Folded Slot Antennas

2.5 Design of Experiment Techniques

Design of Experiment (DOE) techniques are very useful in understanding cause-and-effect relationships in a system, by deliberately changing the input variables to the system and observing the changes in the system outputs that these changes produce [14]. The base of the DOE is the analysis of variance (ANOVA) using the data of the runs. This technique has been previously employed in antenna characterization to understand the effects that the antenna dimensions have in the different antenna parameters, such as resonant frequency, reflection coefficient, and gain, among others. In [15] and [16] inductively-fed and capcitively-fed folded-slot antennas were characterized using DOE techniques. In [15], Cordoba-Erazo, characterized both cases of the folded-slot antenna using the DOE techniques. In this work Cordoba-Erazo characterized the input impedance and resonant frequency of the antenna, as a function of the antenna dimensions as well as the cavity dimensions, at a frequency of 4.5 GHz. In [16], the capacitively-fed configuration had seven variables, as shown in Fig. 4 and operates at 2.4 GHz.

The characterization in [16] was realized using a 2^7 full factorial and 4 center points and intended to characterize the resonant frequency and the return loss of the antenna. The characterization showed that only two of the dimensions had a significant effect in the resonant frequency, and the interaction of some of the dimensions affect the return loss. Using DOE as a characterization technique helps to understand which dimensions of the antenna can be modified to obtain the desired performance and size.

Another work about the use of DOE techniques is presented by Lopez Rivera in [17], in which two resonances and their input impedance for an inductively-fed folded-slot was characterized. The DOE technique employed in this work was a 2^4 factorial. In this work, the resonances characterized were the λ_g and $\frac{3}{2}\lambda_g$, resulting in one dimension having the most significant effect at each resonance, the lower slot width. In [18] a folded-slot log-periodic was also characterized using the DOE techniques. Del-Rio characterizes this antenna with a 2^5 full factorial, looking at the responses of input impedance, gain and the time domain response. The results show that the boom impedance and the boom length are the most significant factors of the antenna in the gain pattern and the impedance bandwidth.

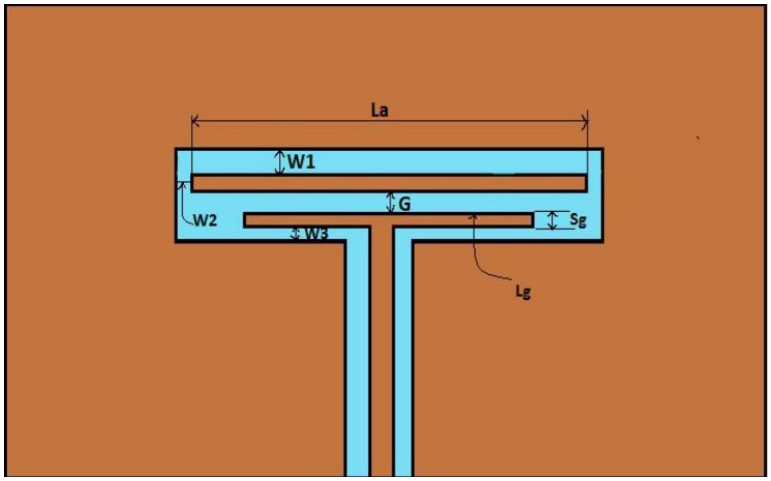

Figure 2.15: Capacitively-Fed Folded Slot Antenna used in [Valentin]

2.6 Summary

This chapter presents several works related to antennas for body centric wireless communication. The chapter presents different antenna configurations and different human body models. This chapter also presents a description of antenna miniaturization techniques to have a better understanding of this process. The works presented in this chapter, and the miniaturization techniques, design of experiments and human modeling, will serve as a guide to complete this thesis. In the next chapter the methodology employed during this work will be discussed.

CHAPTER 3
METHODOLOGY

Two different antenna configurations, microstrip patches and capacitively-fed folded slots, are proposed in this work. The proposed configurations are designed using the Software Ansys High Frequency Structure Simulator (HFSS), which employs the finite element method. The software uses an adaptive refinement of the mesh with a convergence criteria of two percent. To obtain a more stable mesh, a criteria of two consecutive convergence passes are employed to all of the cases proposed in this work. After the adaptive generation of the mesh, the software starts with the solution process. The solution process was selected as an interpolating frequency sweep with a tolerance of 0.5%. A single point discrete run was used for generating the near-field and radiation patterns. Fig 3.1 shows the flowchart of the HFSS solution process, Fig 3.2 shows the flowchart of the frequency interpolating sweep employed by HFSS, both plots are provided by HFSS Online Help. To validate the designs, the simulated results will be compared with the results obtained by measured the fabricated antennas.

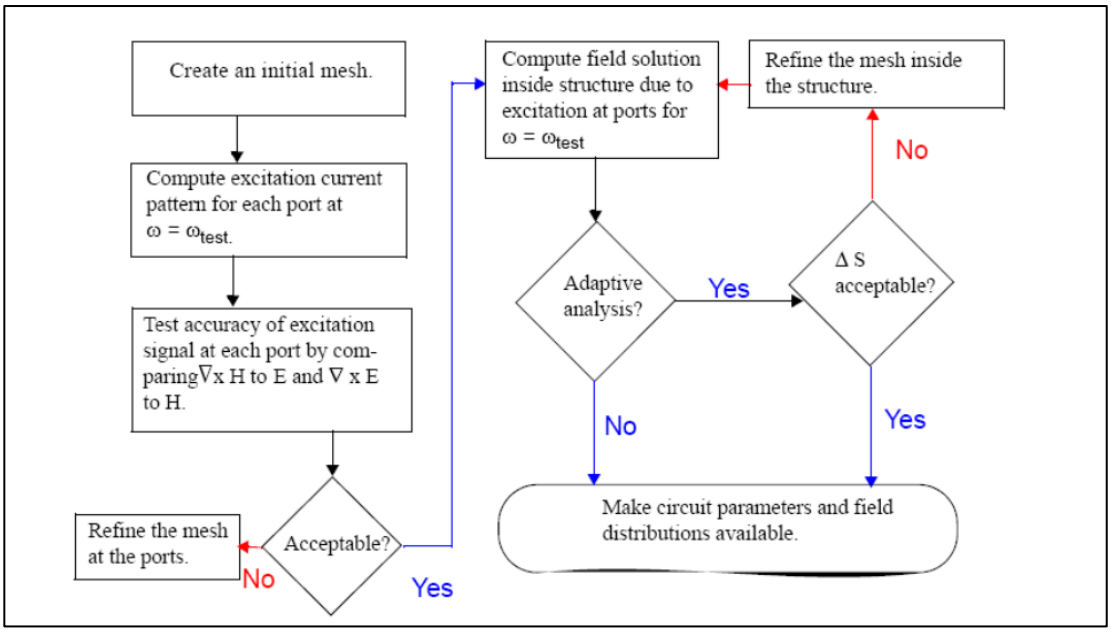

Figure 33.1: Solution Process Employed by HFSS

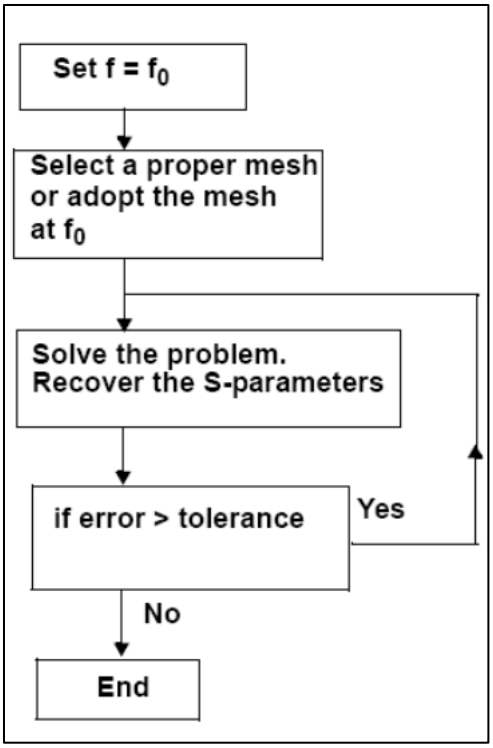

Figure 3.2: Process Employed by HFSS in the Frequency Sweep

3.1 Design Procedure of the Antennas

3.1.1 Capacitively-Fed Folded Slot Antenna

A capacitively-fed folded slot antenna is proposed for this work based on its compact size and to match the inductive effect produced by the substrate integrated cavity described later in this section. This configuration has several design considerations such substrate selection, and cavity type. A Rogers RT/ Duroid 6006 substrate with dielectric constant of 6.15, and thickness of 2.54 mm, was selected for this configuration. This dielectric constant was selected because it will produce a smaller antenna, and the CPW feed dimension are more manageable. In terms of thickness, it was selected because it will produce a higher gain despite the associated size increment. The feed of the antenna is designed to be a 50 Ω coplanar waveguide.

The antenna is backed by a substrate integrated waveguide (SIW) cavity to eliminate the parallel plate modes generated in the substrate, and provide a unidirectional broadside radiation pattern. The cavity dimensions are selected with equation (1), found in Pozar [19], to have their resonant modes out of the 2.4-2.485 GHz band. Table 3.1 shows the three resonant modes of the first resonant frequency of the cavity for the antenna configuration shown in Fig 3.3 with a=43 mm and c=40 mm. In order to validate the baseline antenna, a simulation using method of moment software FEKO was employed. The results agree very well, as shown in Fig 3.4.

$$(f_r)_{mnp}^{TE} = \frac{1}{2\pi\sqrt{\varepsilon\mu}}\sqrt{\left(\frac{m\pi}{a}\right)^2 + \left(\frac{n\pi}{b}\right)^2 + \left(\frac{p\pi}{c}\right)^2} \quad (1)$$

For

$$m = 1,2,3, \ldots$$

$$n = 1,2,3 \ldots$$

$$p = 1,2,3 \ldots$$

$$m = n \neq 0$$

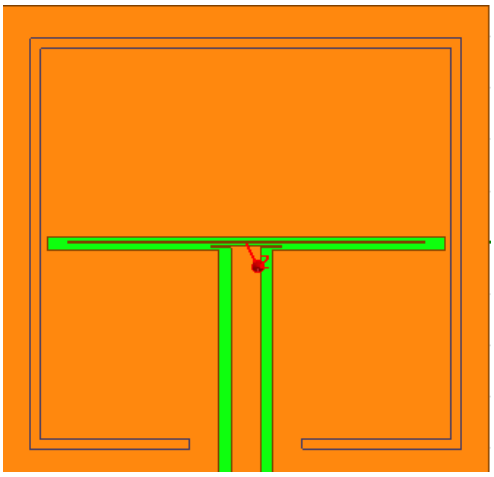

Figure 3.3: Capacitively-Fed Folded Slot Antenna Geometry

Mode	M	N	P		Resonant Frequency (GHz)
TE	1	0	1		2.065246294
TE	1	0	2		3.193933768
TE	1	0	3		4.48268863

Table 3.1: Resonant Frequencies of the Cavity

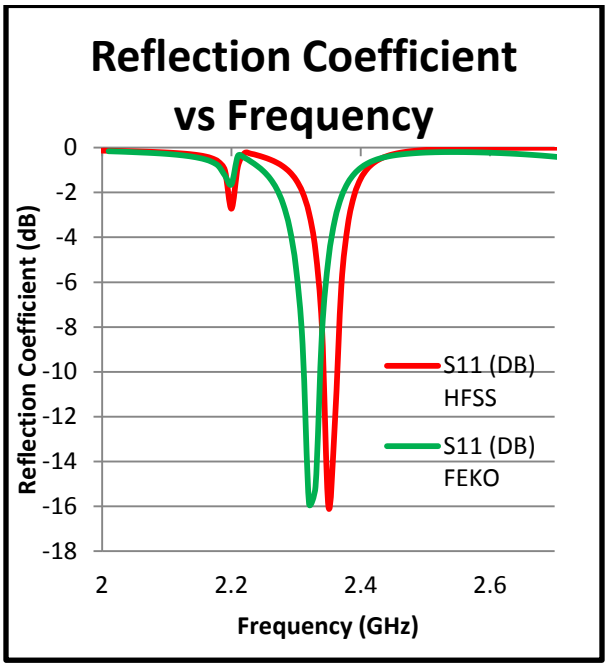

Figure 3.4: Comparison between FEKO (Green) and HFSS (Red) for the capacitively-fed folded slot antenna.

To understand the effects of the dimensions in the resonant frequency and return loss, a characterization using Design of Experiment techniques was performed. The technique used was a 2^k full factorial, which shows the effect of each variable as well the effect of the interaction between them. To employ this technique, a *k* number of variables should be selected. The variable should be evaluated in two levels, to better understand the effect when the variables increase or decrease. This produces a regression model that shows how much effect each variable and each interaction have on the responses.

In this work, the variables are taken as the physical dimensions, and the two levels of the variables were selected to be 10% above and below of the designed baseline antenna physical

dimensions. This results in a total of 128 runs, each run consisting in a simulation in HFSS. Fig 3.5 shows the antenna geometry with the selected factors and each level.

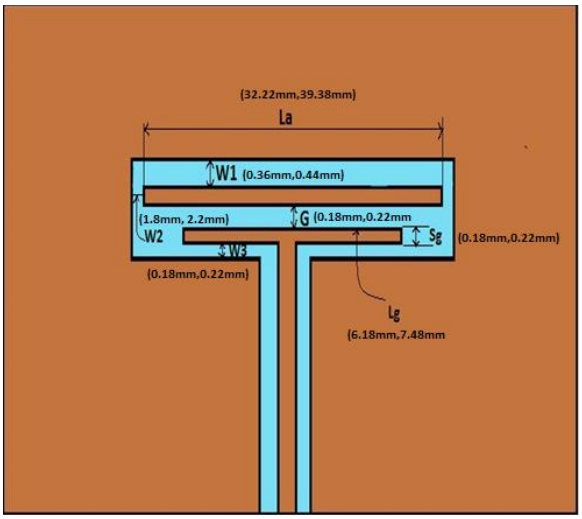

Figure 3.5: Antenna Geometry With the Factors and Levels of the DOE

During each run, the resonant frequency and magnitude of the reflection coefficient were obtained from the plots. The data of the runs, including the results, were statistically analyzed in Minitab. The analysis of variance (ANOVA) and the half normal probability plot were used to see which of the variables has a direct effect in the selected responses as well which interaction. A reliability of 99% was used in the characterization, which implies a 1% of unexpected error.

3.1.2 Modified Capacitively-Fed Folded Slot Antenna

A modification to the original capacitively-fed antenna was employed to obtain a smaller antenna. To achieve it, a modification in the cavity and a miniaturization technique were employed. It was observed that the cavity dimensions have an effect on the resonant frequency. It was observed that reducing the cavity size had the effect of increasing the resonant frequency of the antenna. Therefore, to keep the ground plane size small, the cavity was implemented by a

solid copper wall around the substrate, instead of the SIW wall. This cavity type keeps its resonant modes out of the operation band and allows a smaller size of the antenna.

The loading slot technique discussed in [10] was employed to reduce the antenna size, adding a total of eight loading slots. This creates a larger path to the magnetic current, which allows the reduction of the antenna length. Fig 3.6 and Fig 3.7 shows the antenna geometry and the electrical current distribution at the metal surface of the modified antenna, respectively. The cavity walls in this configuration were solid copper around the substrate. The ground plane of the antenna was designed to be 40 mm by 40 mm to improve the radiation pattern of the antenna and to make it unidirectional. This selection of ground plane size was based on work by Chandran ,et. al. in [8].

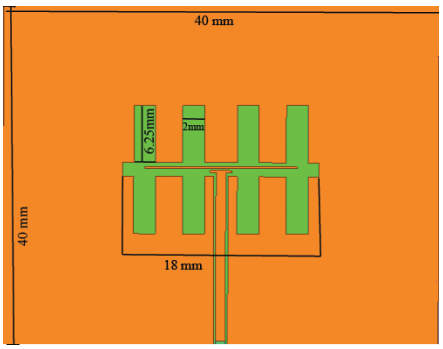

Figure 3.6: Modified Antenna Geometry

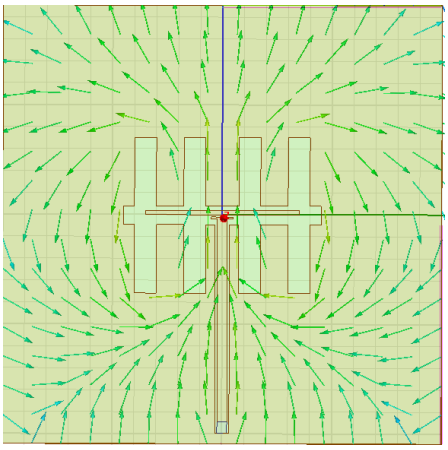

Figure 3.7: Electrical current distribution on the slot plane

Since the bandwidth of this configuration is less than the 85 MHz required, some modifications were employed. First, a selection of new substrate with a lower dielectric constant was performed. To make the antenna functional with the new substrate, the dimensions of the original antenna were scaled. Another technique employed was an offset of the antenna. The offset was taken from the center of the cavity to reduce the input impedance and improve the bandwidth. Fig 3.8 shows the geometry with the offset. All of these techniques were employed and compared with the original, to see the change in bandwidth.

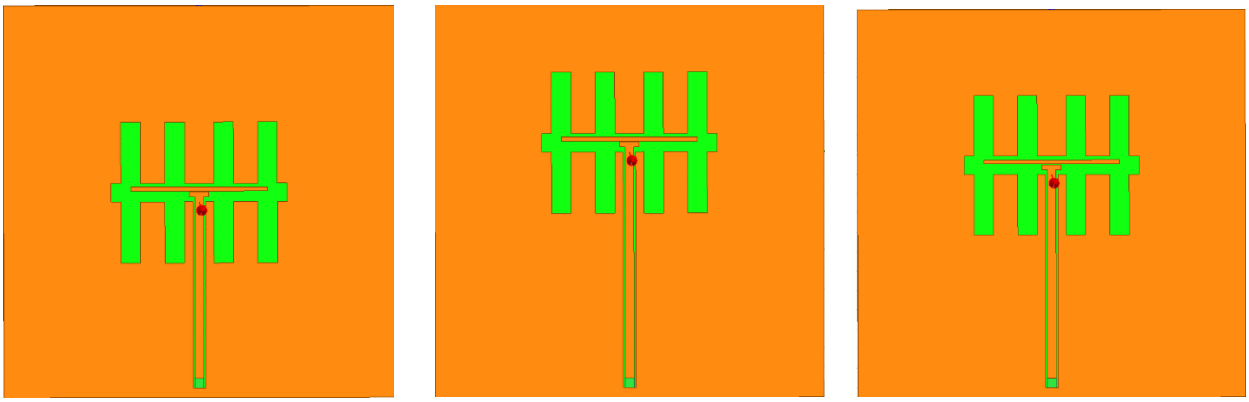

(a) (b) (c)

Figure 3.8 Offset Employed (a) Original (b) offset of 5 mm (c) offset of 3 mm

3.1.3 Rectangular Patch Antenna

A rectangular patch antenna is also proposed. The patch is designed on a Rogers RT/ Duroid 6006 substrate with a thickness of 2.54 mm. This substrate selection was made based in the same considerations of mentioned in part 3.1.1. A microstrip line feed was chosen, using an inset feed for impedance matching. Since a small antenna is desired, the use of matching networks like stubs, or quarter wave transformer is limited.

The initial dimensions of the patch were chosen by transmission line method. The dimensions obtained were 25 mm by 25 mm. For this configuration, a 40 mm by 40 mm ground plane is used. To reduce the size of the patch, five vias were placed at the edge to make the patch a quarter wave structure, reducing the patch dimensions to 12.5 mm by 25 mm. This is possible due to the electric field distribution on the patch, which becomes virtually zero at the center of the patch. Fig 3.9 shows the electric field distribution of the original patch.

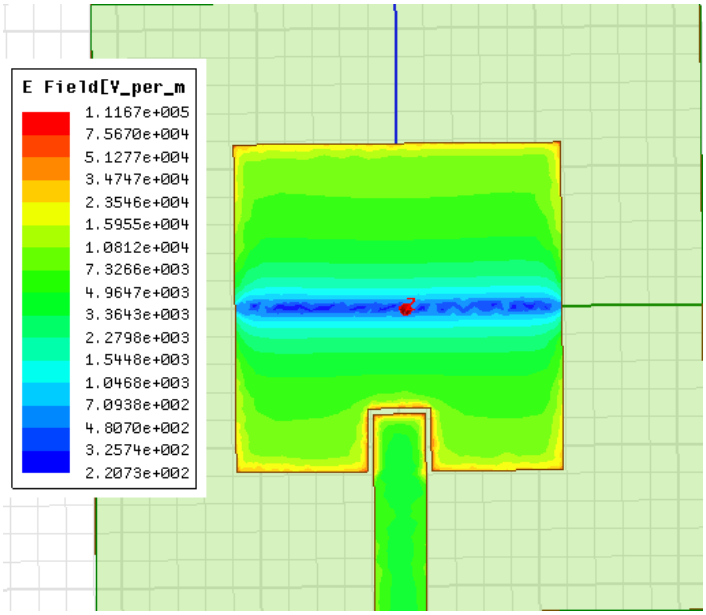

Figure 3.9: Electric Field Distribution of the Original Rectangular Patch

To further reduce the size of the patch, the slot loading technique discussed in [10] was employed. Three loading slots were placed based on the current flow at the patch to reduce the patch length. With this technique the patch is further reduced to 10.5 mm by 25 mm. The ground plane of the antenna was selected to be 40 mm by 40 mm to reduce edge effects and maintain a unidirectional radiation pattern. Fig 3.10 shows the antenna geometry with the associated dimensions.

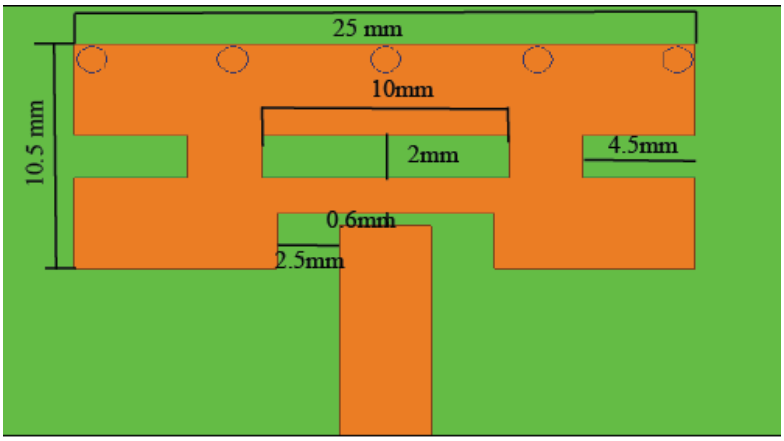

Figure 3.10: Modified Patch Geometry

To improve the bandwidth and fit the 2.4-2.485 GHz band, a parasitic patch is placed in the same plane of the feed patch. The parasitic patch is designed to be also a quarter-wave structure and have the three loading slots. This configuration was tested and provided a bandwidth of around 50 MHz. To obtain the desired bandwidth, a substrate with a lower dielectric constant should be used. The dimensions of the configuration in the Rogers 6006 were scaled to obtain a similar performance in a Rogers Duroid 5880 with a thickness of 3.175 mm. In this case, the bandwidth was reached. Fig 3.11 shows the configuration of the parasitic rectangular patch antenna.

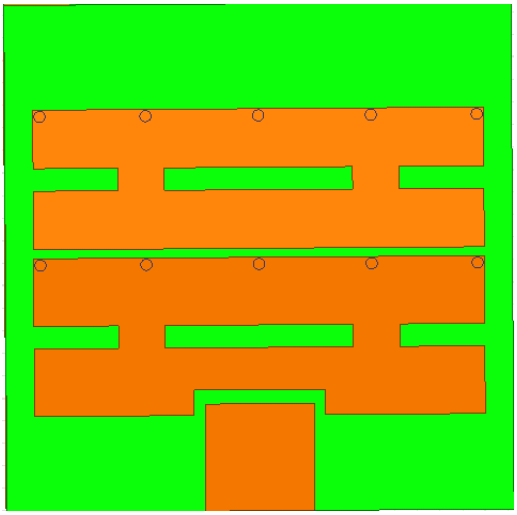

Figure 3.11: Parasitic Rectangular Patch Configuration

3.2 Human Body Model

A simple model of the human body in the desired frequency band was developed as a uniform layer model. A cylinder with radio of 45.8mm and length of 124mm, which simulates a forearm, was the shape used for the model. The electromagnetic properties of the material were calculated as a weighted average of the different tissues, using the values from, P.Hall and Y.Hao [5]. Equation (2) was used in the calculation of the dielectric constant. Equations (3) & (4) were used to calculate the conductivity and loss tangent, respectively. To verify that there are no mesh problems with this model, a simulation with an air cylinder, with the same dimensions as the one previously mentioned, was performed and compared with the simulation with antenna without the cylinder. Once verified that the same results is obtained in both cases, the simulation with the cylinder with the calculated electrical parameters was performed.

$$\varepsilon_{rModel} = Fat\% * \varepsilon_{rFat} + Muscle\% * \varepsilon_{rMuscle} + Bone\% * \varepsilon_{rBone} + Skin\% * \varepsilon_{rSkin} + Blood\% * \varepsilon_{rBlood} \quad (2)$$

$$\sigma_{Model} = Fat\% * \sigma_{Fat} + Muscle\% * \sigma_{Muscle} + Bone\% * \sigma_{Bone} + Skin\% * \sigma_{Skin} + Blood\% * \sigma_{Blood} \quad (3)$$

$$\tan\theta_{Model} = Fat\% * \tan\theta_{Fat} + Muscle\% * \tan\theta_{Muscle} + Bone\% * \tan\theta_{Bone} + Skin\% * \tan\theta_{Skin} + Blood\% * \tan\theta_{Blood} \quad (4)$$

The model was simulated in HFSS with the radiation boundary at the edge of the cylinder length, to simulate the cylinder as an infinitely long structure. The uniform cylinder model was compared with a five-layer model and the same results were obtained. Another advantage seen

in the uniform cylinder model, is that it required 33% less computational time. Fig 3.12 shows the electric field distribution of the proposed model with the antenna.

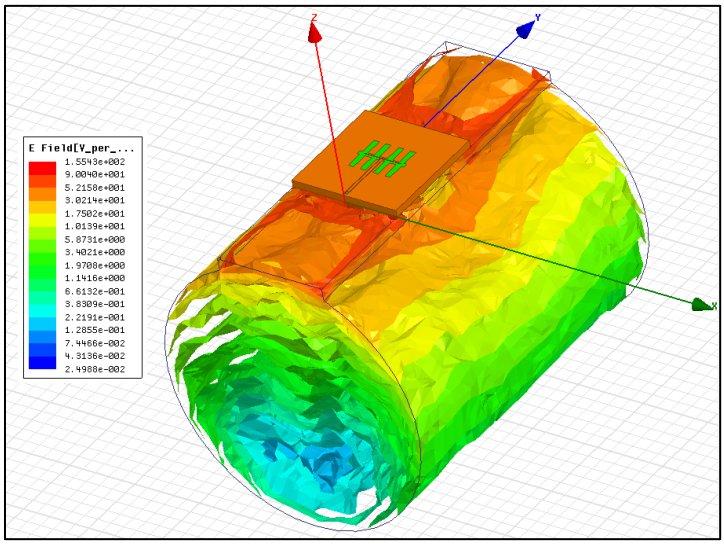

Figure 3.12: Electric Field Distribution of the Proposed Uniform Layer Model

3.3 Experimental Validation

The antennas were fabricated using a *LPKF ProtoMat H100* milling machine. After the process in the milling machine, the shorting pins for the patch and the SIW cavity are placed. The shorting pins were made with fine copper wire, and the SIW cavity was done with copper rivets. In case of the cavity with a solid wall of copper, the cavity walls were made with copper tape, after removing the adhesive with alcohol, and soldered in the antenna grounds. Fig 3.13 shows an example of the fabricated antennas with a solid wall cavity, and Fig 3.14 shows the SIW cavity.

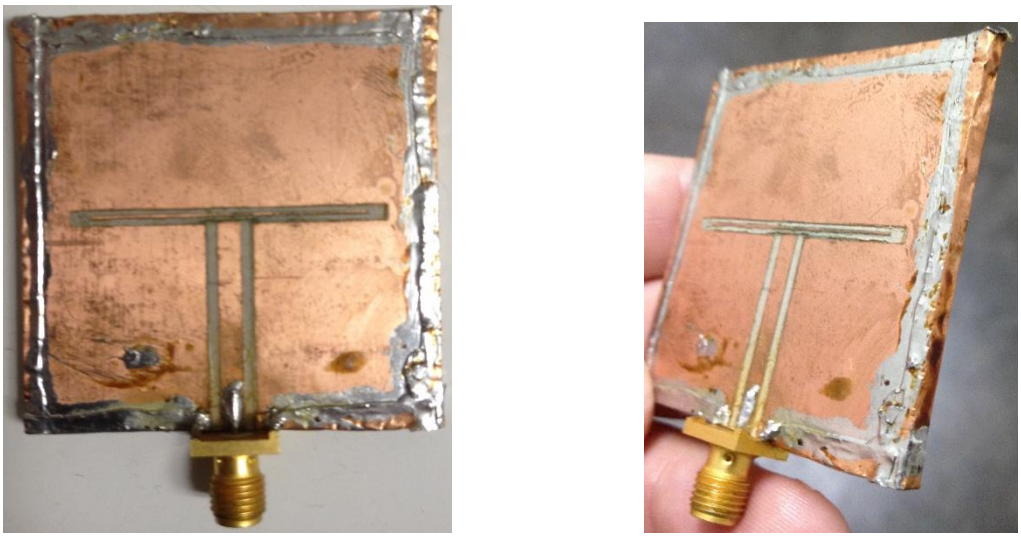

(a) **(b)**

Figure 3.43: Top View of the Fabricated Capacitively-Fed Folded Slot Antenna With the Solid Wall of Copper Cavity Type (a) and Side View of the Same Antenna (b)

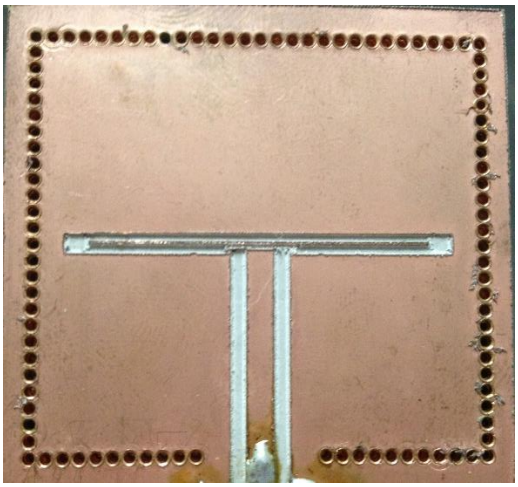

Figure 3.14: Top View of the Fabricated Capacitively-Fed Folded Slot Antenna With the Substrate Integrated Cavity Type

Having the fabricated antennas, the impedance and reflection coefficient were measured in the UPRM Microwave and Millimeter-Wave System Laboratory with an *Agilent PNA N5227A* network analyzer. The radiation gain pattern was measured in the anechoic chamber in the University of Colorado at Boulder. The measured results were compared with the simulation results to validate the antennas. In the next chapter, the results of both simulations and measurements will be shown.

CHAPTER 4
RESULTS AND DISCUSSION

This chapter presents the results for the antennas described in Chapter 3. The chapter is divided in five parts. The first section presents the results of the capacitively-fed folded slot antenna, including the characterization with the DOE technique. The next three sections present the results of the other configurations; the modified capacitively-fed folded slot antenna, rectangular patch, and the parasitic patch. The final section presents the result of the antennas using the model of the human body presented in Chapter 3.

4.1 Capacitively-Fed Folded Slot Antennas

As mentioned in Chapter 3, this antenna was simulated using HFSS, which produces the plots of input impedance, reflection coefficient, and radiation pattern. The plots were taken in a sweep from 2.0 GHz to 2.6 GHz. In terms of input impedance and reflection coefficient, the plots show a spike in 2.2 GHz. This spike is due to the resonance of the first mode propagated in the cavity. Figs 4.1 and 4.2 show the results in terms of input impedance and reflection coefficient, respectively. The bandwidth is about 20MHz.

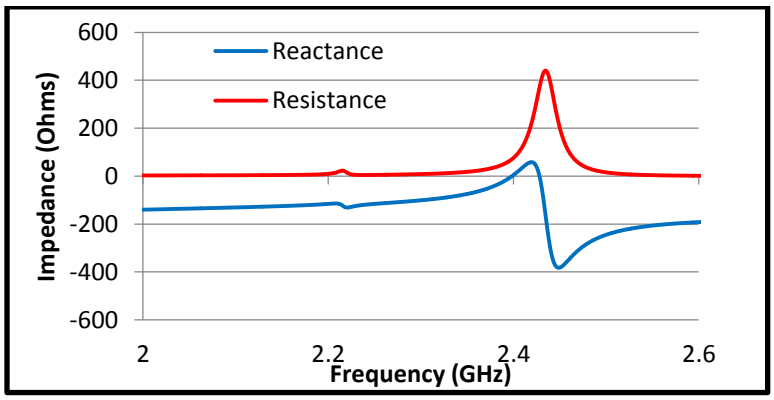

Figure 4.5: Input Impedance of the Capacitively-Fed Folded Slot Antenna Imaginary part (blue) Real Part (Red)

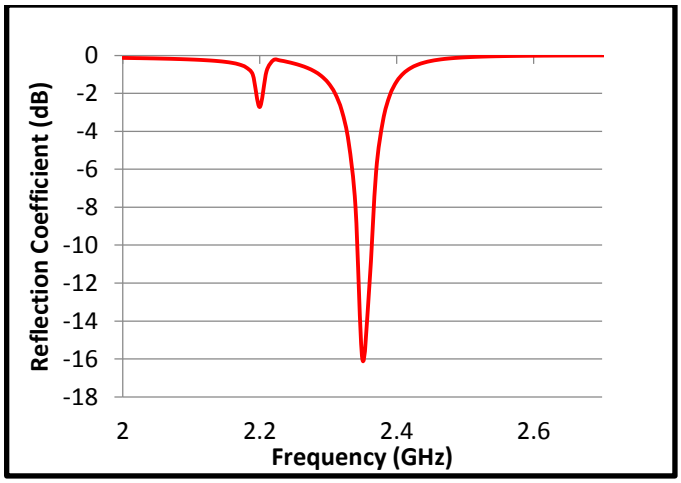

Figure 4.2: Reflection Coefficient of the Capacitively- Fed Folded Slot Antenna

As mentioned in Chapter 3, a characterization of this antenna was performed using DoE. The characterization shows that only two of the dimensions affect the resonant frequency of the antenna. The two dimensions that have the main effect in the resonant frequency were La and Lg, which are the length of the antenna and the length of the capacitive feed respectively. In terms of the reflection coefficient, the same variables have the main effects in this response, but now interactions with other variables. This data was obtained from the half-normal plots produced in Minitab. This plot shows statistically the variables that affect the responses. Fig 4.3 and 4.4 show the half-normal plot for resonant frequency a reflection coefficient.

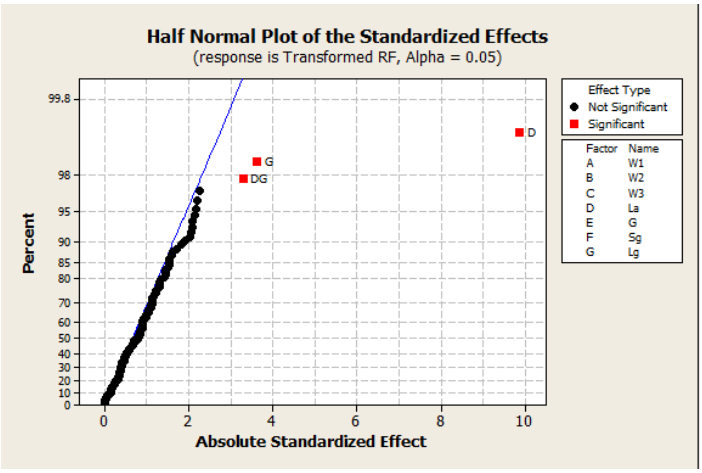

Figure 4.3: Half Normal Plot for Resonant Frequency

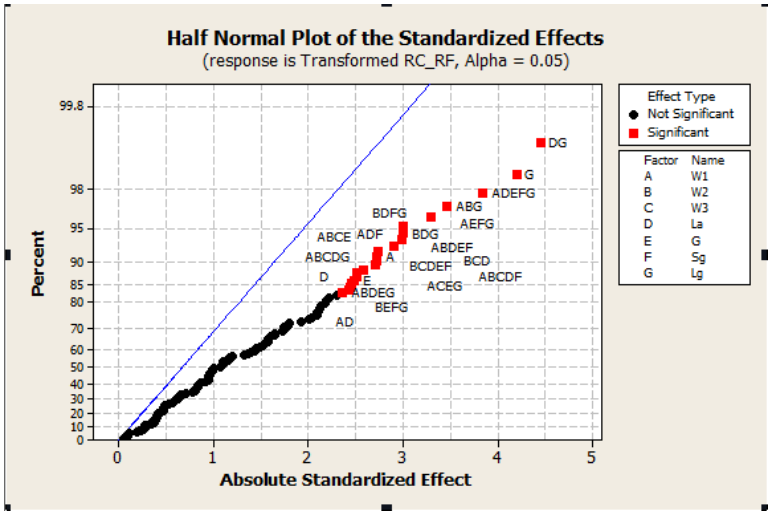

Figure 4.4: Half Normal Plot for Reflection Coefficient

In terms of resonant frequency, the variable which has more effects is *La*, this variable controls the perimeter of the antenna which produce the current path, then it directly affects the resonance. Fig 4.5 shows a plot of reactance that explains the effect of *La* in the resonant frequency. This plot shows that if *La* increases, the resonant frequency decreases. This is due to the increment in the current path produced by the increment in *La*.

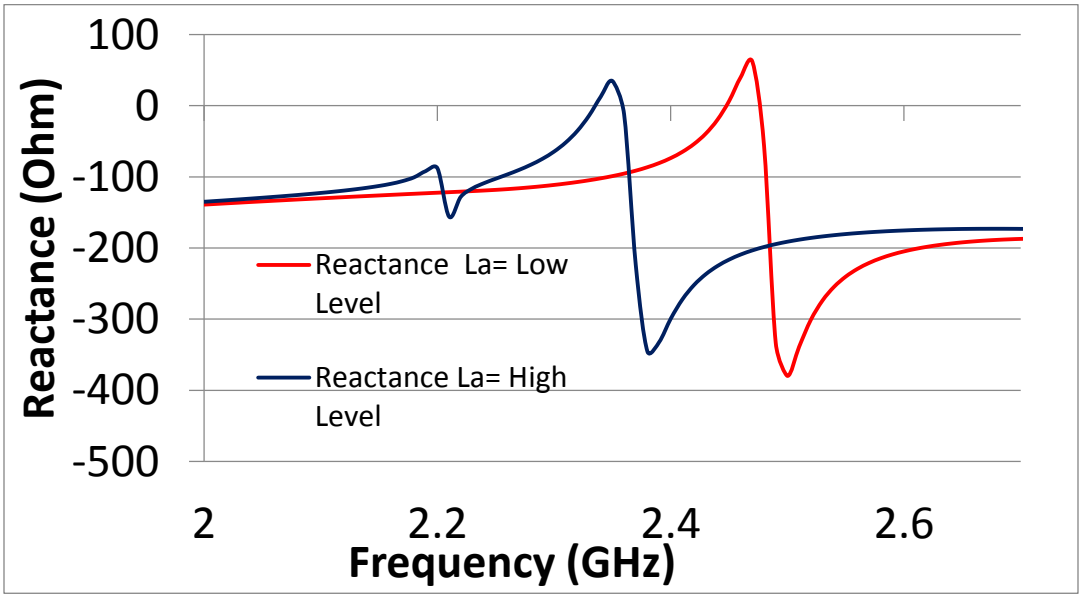

Figure 4.5: Comparison in Reactance by Change in La in High Level (blue) and Low level (red)

The second dimension that has a major effect in resonant frequency is Lg. This dimension controls the capacitance of the capacitive coupling of the feed. Fig 4.6 shows a plot of reactance explaining the effect of this dimension. As *Lg* increases, the magnitude of the reactance decreases, as well the resonant frequency.

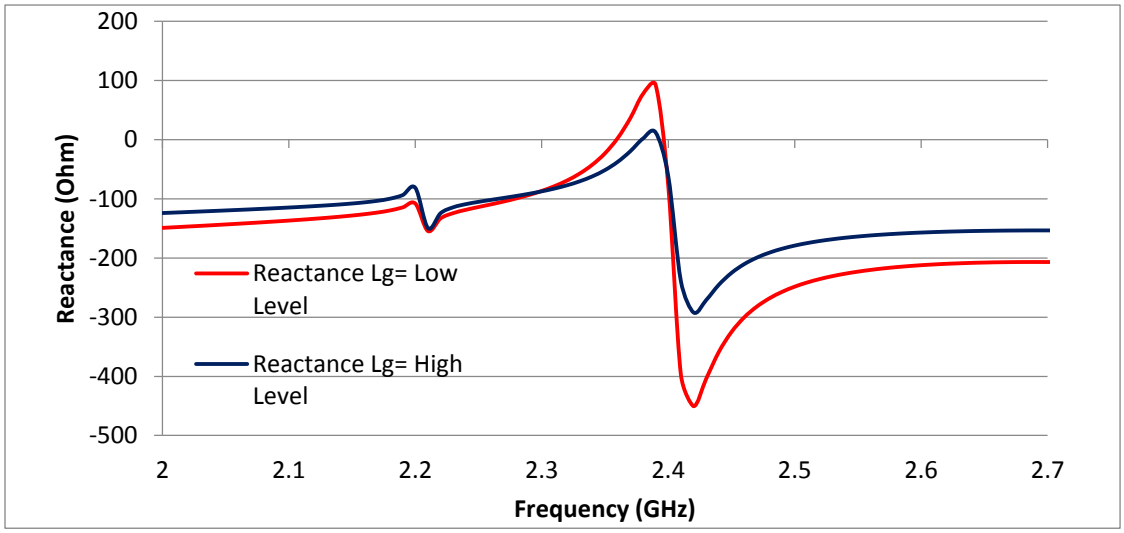

Figure 4.6 Reactance Comparison by a Change in Lg at High Level (blue) and Low Level (red)

In terms of reflection coefficient, it is affected by an interaction between *La* and *Lg* with other variables, as shown in Fig 4.4. *Lg* has the larger effect, as shown in Fig 4.4. The main interaction is the one between *Lg* and *La*, it can be explained because this two controls the capacitively effect of the fed which is related with the input impedance of the antenna. The main effect of *Lg* can be explained by the effect in the magnitude of the reactance. The effects are mostly interactions of *Lg* and the slot widths, all of which control the magnitude of the input impedance.

4.2 Cavity Type Modification

It was observed that, as the size of the cavity was reduced, the resonance of the antenna moves to a higher frequency, which results in a larger size of the antenna for operation in the desired band. Due to this effect, a change in the implementation of the cavity from substrate integrated cavity wall to a solid copper wall around the substrate was performed. The Fig 4.7 shows the reflection coefficient comparison between the two types with a dimension of 43 mm by 40 mm in both cases.

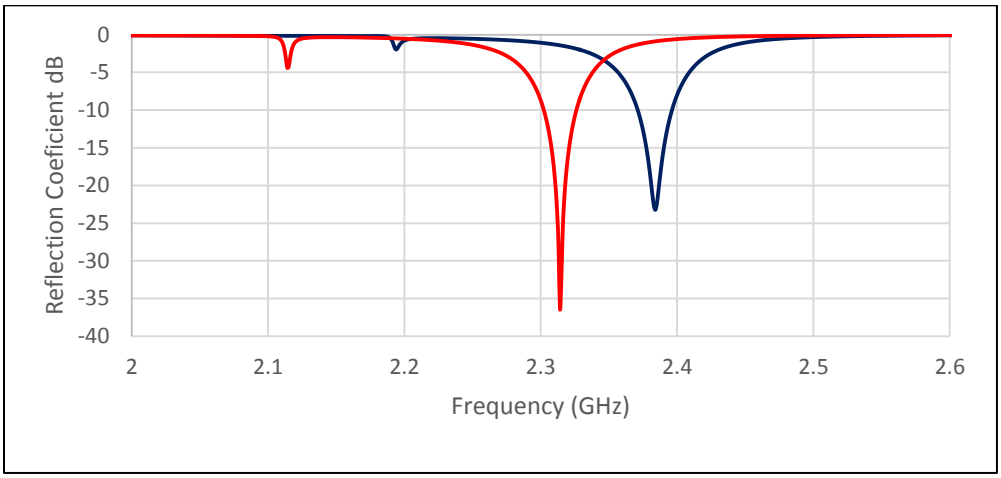

Figure 4.7: Reflection Coefficient Comparison Between Substrate Integrated (Blue Line) and the Solid Copper Wall (Red)

Using the cavity as a solid wall of copper, a 43 mm by 40 mm ground plane, the resonant frequency of the antenna was reduced by 70 MHz compared with the SIW cavity of 43 mm by 40 mm in a 47.5 mm by 47.5 mm ground plane. In terms of gain pattern, the SIW type results in 1.2 dB more gain and 1.5 dB better front to back ratio. This can be explained because the SIW type has a larger ground plane than the solid wall type. Fig 4.8 shows the comparison between their radiation patterns.

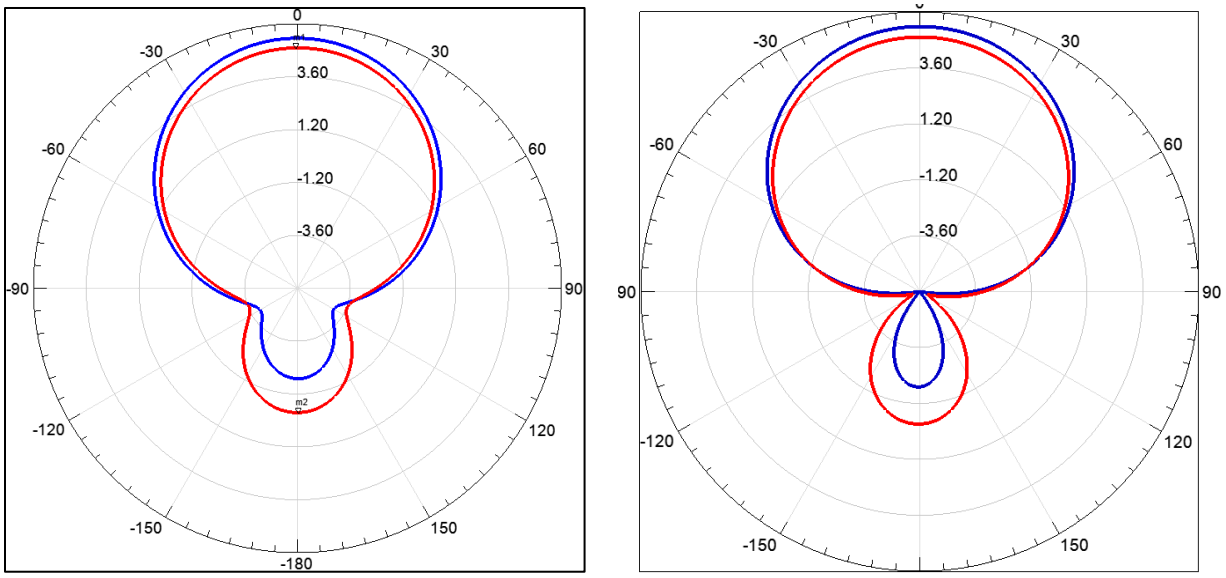

(a) (b)

Figure 4.8: Simulated Gain Pattern Comparison between SIW Cavity (blue) and Solid Wall of Copper Cavity (red), in H-Plane (a) and E-Plane (b)

With these results, it was decided to make the copper foil type cavity as the same ground plane size of the antenna with the SIW type. This resulted in a better gain pattern with the same gain, 0.7 dB better front to back ratio, and a resonant frequency of 20 MHz lower. Fig 4.9 and Fig 4.10 shows the comparison between these antennas in reflection coefficient and radiation pattern.

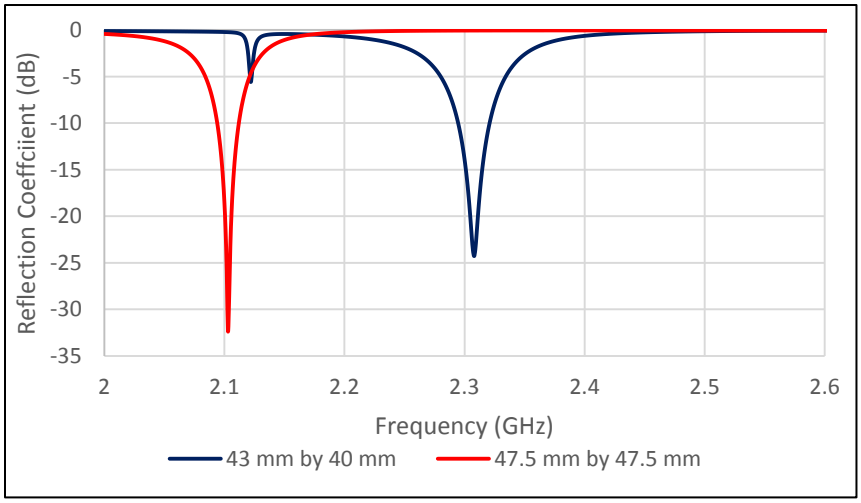

Figure 4.9: Reflection Coefficient Comparison of the Solid Wall of Copper with a size of 43 mm by 40 mm (blue) and 47.5 mm by 47.5 mm (red)

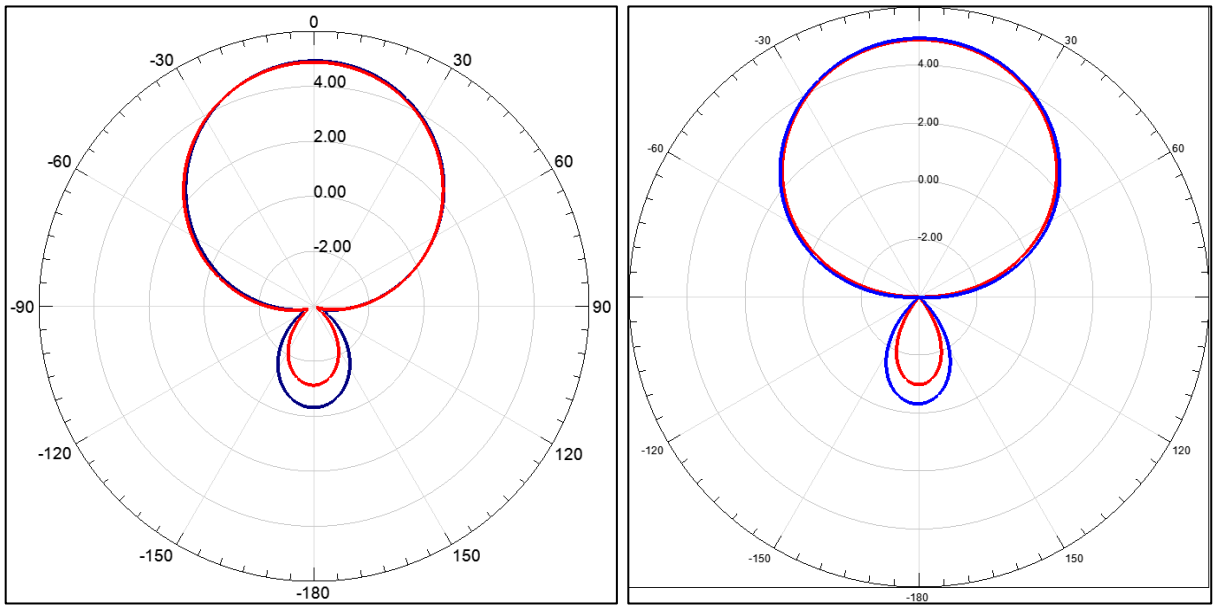

(a) (b)

Figure 4.10: Simulated Gain Patter Comparison of the Solid Wall of Copper with a size of 43 mm by 40 mm (blue) and 47.5 mm by 47.5 mm (red), in H-Plane (a) and E-Plane (b)

4.3 Modified Capacitively-Fed Folded Slot Antennas

With the new cavity type, another modification was performed to reduce the size. The loading slot technique was employed, adding eight loading slots to the antenna. As mentioned previously, this technique will increment the current path, producing a smaller antenna. This modified configuration allows an antenna with a ground plane of 27.5 mm by 27.5 mm and a has a length of 24 mm. The behavior of the antenna is similar to the original, but with less gain and front to back ratio. Now the front gain becomes 2.98 dB with a front to back ratio of 2.22 dB. For the application of BCWC a larger front-to-back ratio would be desired. Fig 4.11 and Fig. 4.12 show the radiation pattern of this new configuration and its reflection coefficient, respectively.

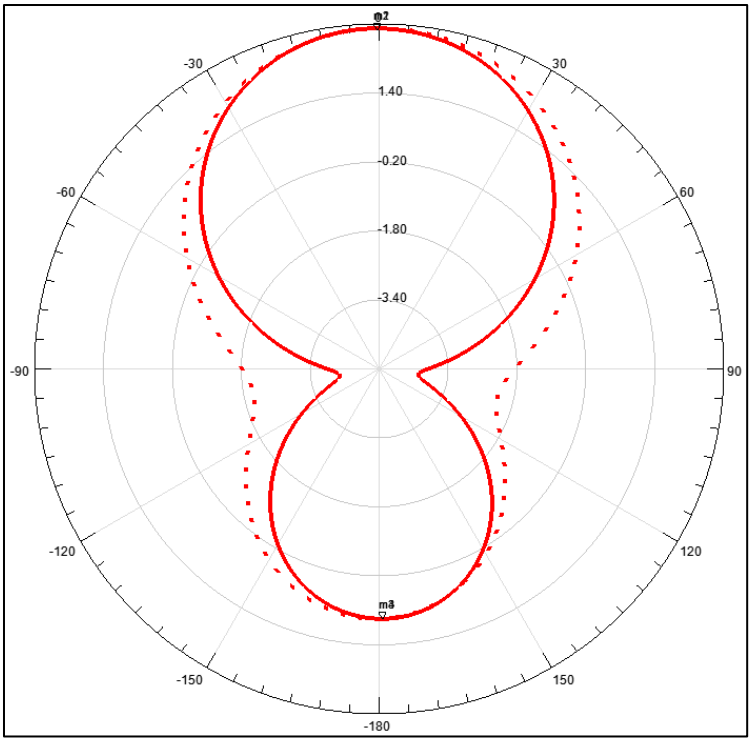

Figure 4.11: Simulated Radiation Pattern in, H-Plane (solid) and E-Plane (dot) of the modified capacitively-fed folded slot antenna with a ground plane size of 27.5 mm by 27.5 mm

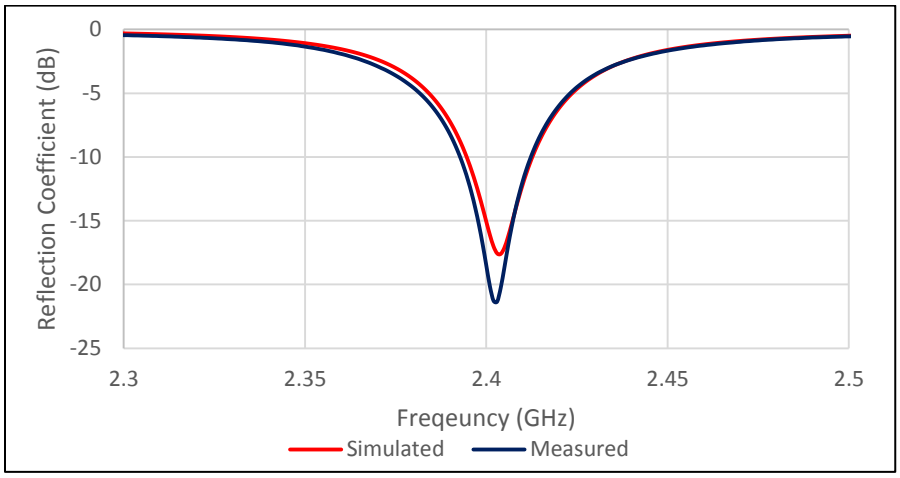

Figure 4.12 Reflection Coefficient Comparison between the Simulated Result (red) and Measured Results (blue) of the Modified Capacitively-Fed Folded Slot Antenna in a Ground Plane of 27.5mm by 27.5mm

Due to this result in terms of radiation pattern, the size of the ground plane was increased to be 40 mm by 40 mm. With this design, the front gain becomes 4.27 dB with a front to back

ratio of 5.16 dB. The antenna length was also reduced in size, now the length of the antenna is 16 mm. The reflection coefficient has only 5 MHz of difference comparing both ground plane size. Fig 4.13 shows the reflection coefficient of this configuration; simulated and measured. The radiation pattern is shown in Fig 4.14.

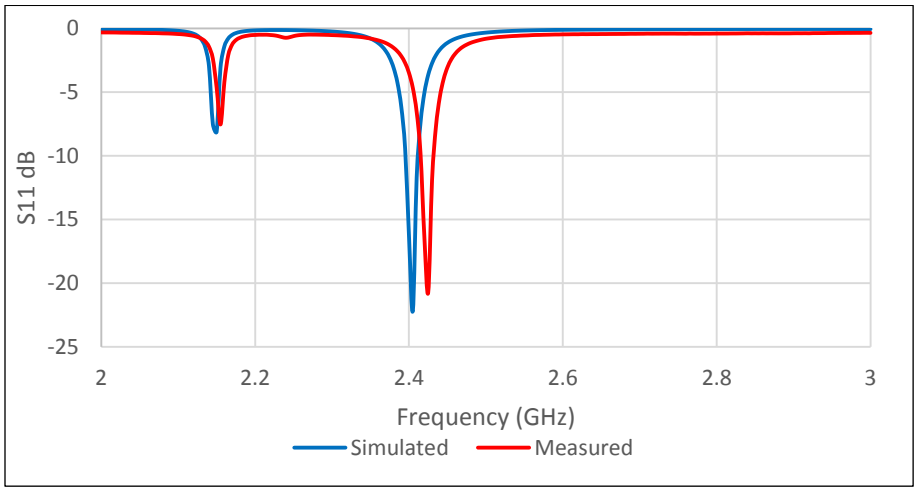

Figure 4.13 Reflection Coefficient Comparison between Simulated Result (blue) and Measured Result (red) of the Modified Capacitively-Fed Folded Slot Antenna with a Ground Plane Size of 40 mm by 40 mm.

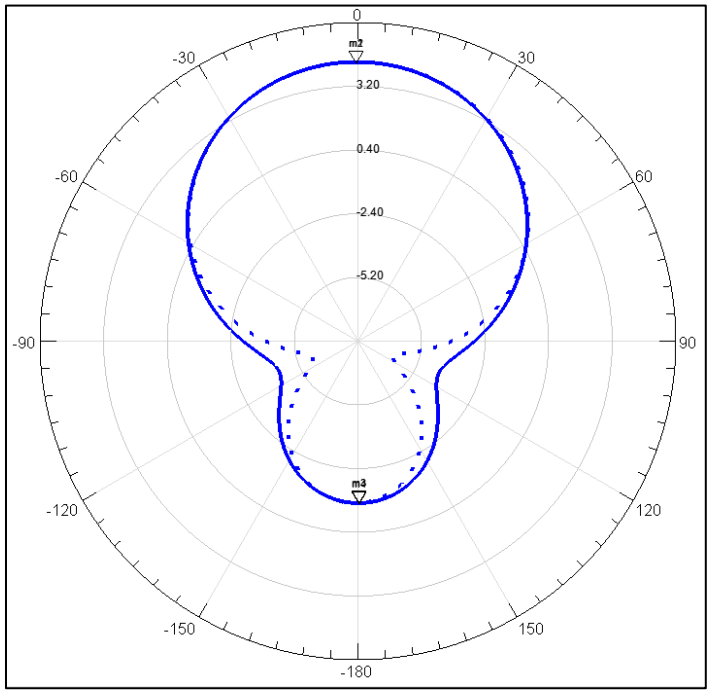

Figure 4.14: Simulated Radiation Pattern in H-Plane (Solid) and E-Plane (Dot) of the Modified Capacitively-Fed Folded Slot Antenna with a Ground Plane Size of 40 mm by 40 mm.

As shown and analyzed in the previous sections, this configuration has a good performance that satisfies the requirements for the application except for the bandwidth. As mentioned in Chapter 3, some techniques for increase the bandwidth were employed. First an offset from the center of the antenna was analyzed. The offset consist in separate the whole antenna from the center of the substrate to an upper position in case of the positive offset, and to a lower positon in case of the negatives. This offset produce only a change in frequency and the desired bandwidth was not achieved. Fig 4.15 shows a parametric analysis with at different offsets.

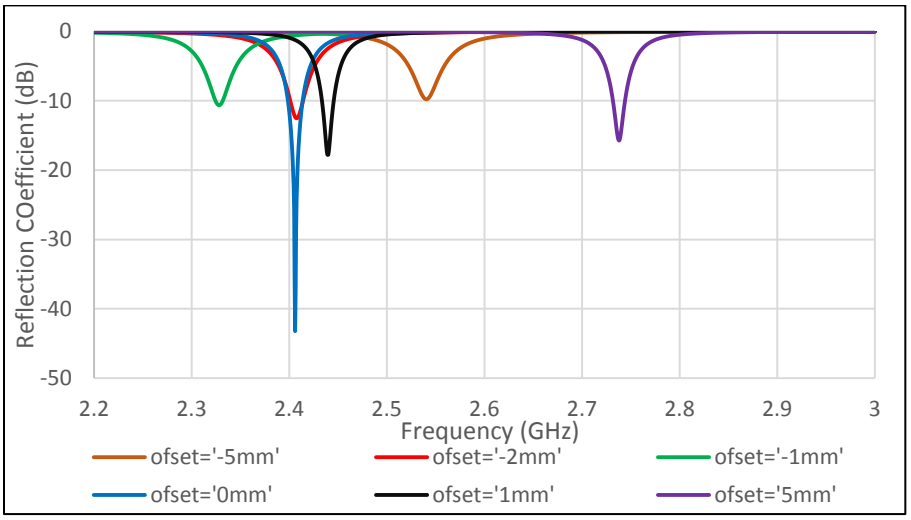

Figure 4.15 Parametric Analysis of the Offset

Another change employed was a change in the substrate. This time the substrate selected was a Rogers 4003 with a dielectric constant of 3.55 and a thickness of 1.524 mm. The bandwidth obtained was 22 MHz which compares with previous works in slot antennas. Fig 4.16 shows the reflection coefficient of the antenna with this dielectric constant.

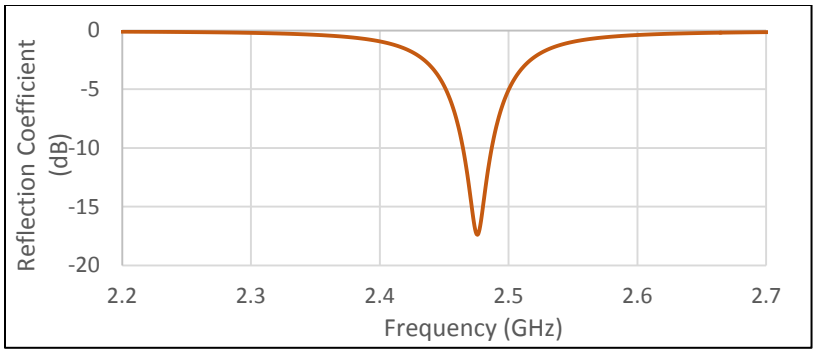

Figure 4.16 Reflection Coefficient with new substrate

4.4 Rectangular Patch

The rectangular patch was designed as a quarter-wave structure. It was achieved by adding five shorting pins at the center of the original patch. To reduce the size of the patch, tree loading slots were added to the patch reducing the length from 25 mm to 10.5 mm in a Rogers RT/Duroid 6006 substrate. This configuration shows a good performance in terms of impedance and reflection coefficient, and also a good radiation pattern. Fig. 4.17 shows a comparison in the reflection coefficient of the patch between the simulated and the measured case. The radiation pattern is shown in Fig. 4.18. The configuration has a front gain of 4.35 dB with a front to back ratio of 5.6 dB, and a bandwidth of 25 MHz.

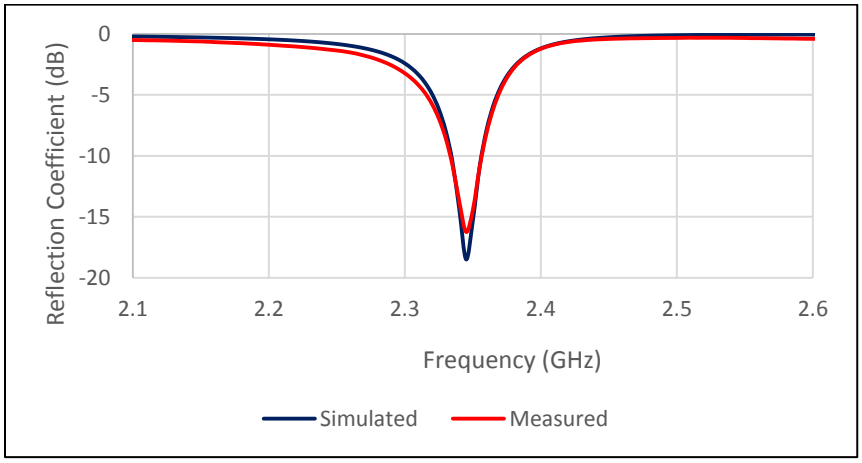

Figure 4.17: Reflection Coefficient Comparison between Simulated Results (blue) and Measured Results (red) of the Rectangular Patch in a Rogers RO 6006

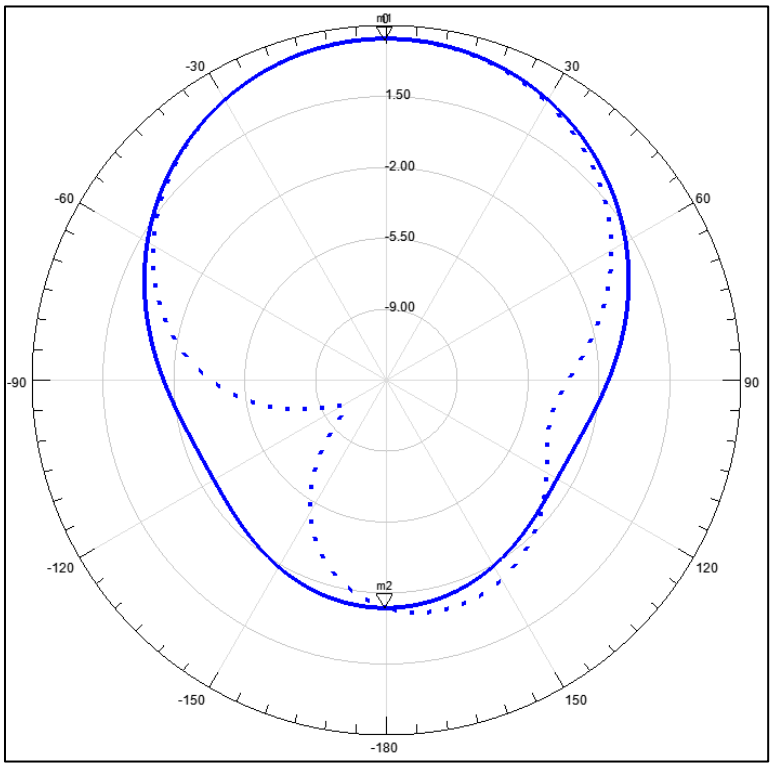

Figure 4.18: Simulated Radiation Pattern, in H-Plane (Solid) and E-Plane (Dot) of the Rectangular Patch in a Rogers RO 6006

As shown in Fig 4.17, the required bandwidth was not achieved in this configuration. To improve the bandwidth, a parasitic patch was added. This parasitic patch was also a quarter-wave structure, and was placed on the same substrate. The configuration shows a bandwidth of 50 MHz, still smaller than the required 85 MHz. Fig 4.19 shows the reflection coefficient of this configuration.

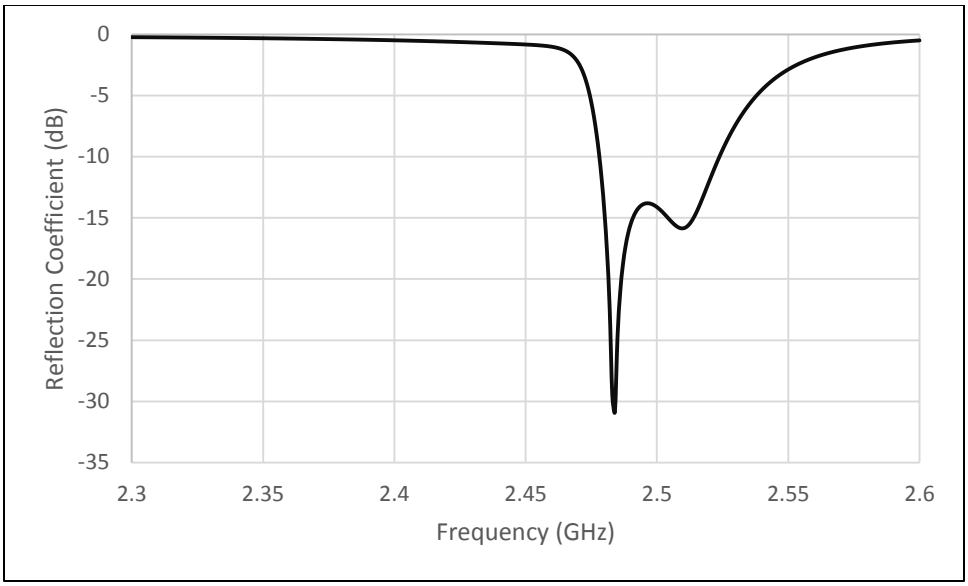

Figure 4.19 Reflection Coefficient Parasitic Patch Rogers 6006

The parasitic patch configuration was scaled and placed on a Rogers RT/Duroid 5880 with a thickness of 3.175 mm and dielectric constant of 2.2. With this substrate the desired bandwidth was reached. A meshing problem in HFSS was detected when the antenna was fabricated the first time, due to disagreement between measurement and simulations. The meshing problem was due to the high coupling in the region between the patches. To improve the model, an air box of 115 mm long, 45 mm wide, and 3.175 mm thick was placed on top of the substrate (on the patch size) to produce a denser mesh on top of the patches. Fig 4.20 compares the simulated and the measured cases for the parasitic patch configuration. Note that the bandwidth is 90 MHz.

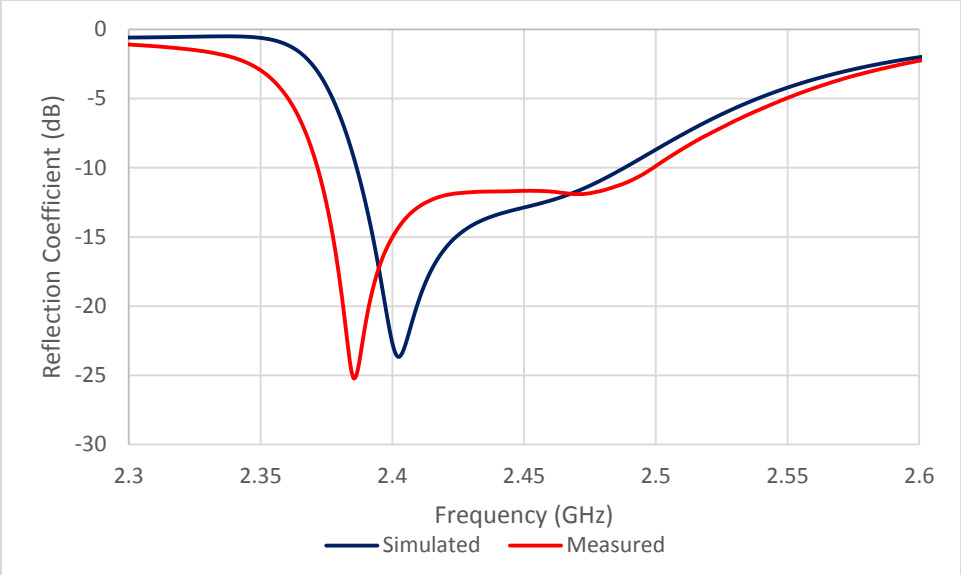

Figure 4.20 Reflection Coefficient Comparison between the Simulated (Blue) and Measured (Red) Results for the Parasitic Patch Configuration

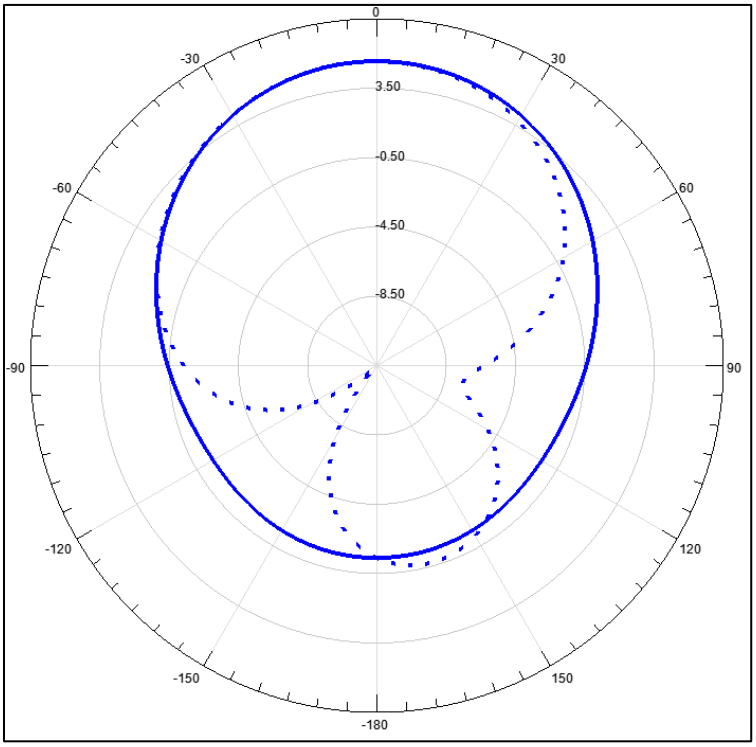

Figure 4.21 Simulated Radiation Pattern in, H-Plane (solid) and E-Plane (Dot), for the Parasitic Patch Configuration

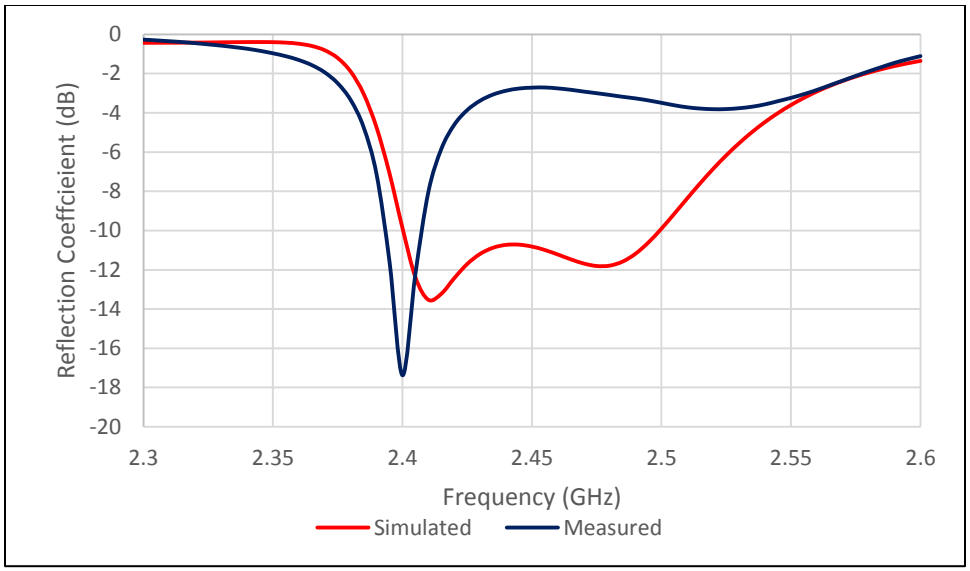

Figure 4.22: Simulated (red) vs Measured (blue) reflection coefficient for the first parasitic patch prototype

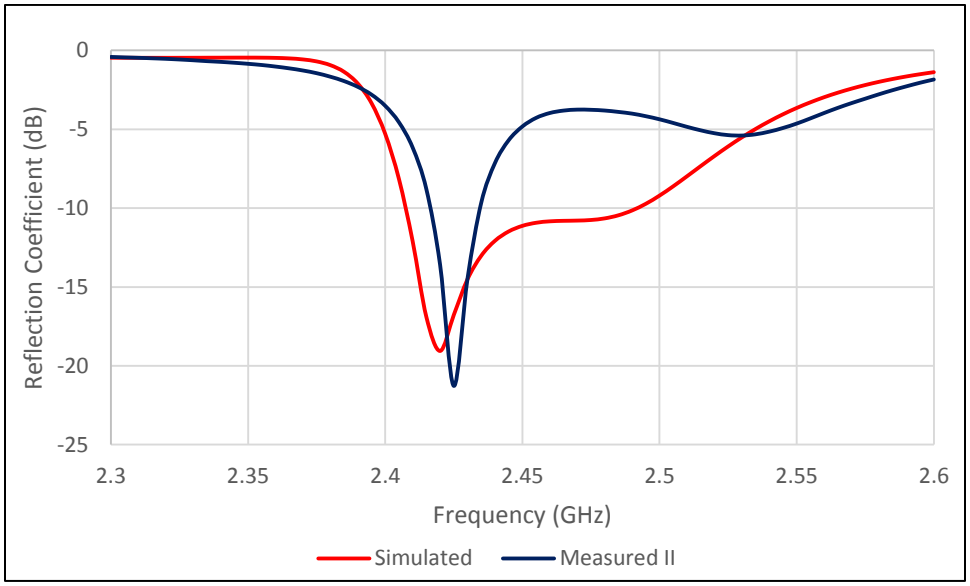

Figure 4.23: Simulated (red) vs Measured (blue) reflection coefficient for the second parasitic patch prototype

4.5 Simple Model of the Human Body

As described in Chapter 3, a uniform cylinder human tissue model was developed to calculate the effect in the antenna performance. First, a simulation using free space in the human

tissue model was conducted. This simulation proves that the mesh problem was calculated correctly. Fig 4.23 shows a comparison in reflection coefficient between these two cases.

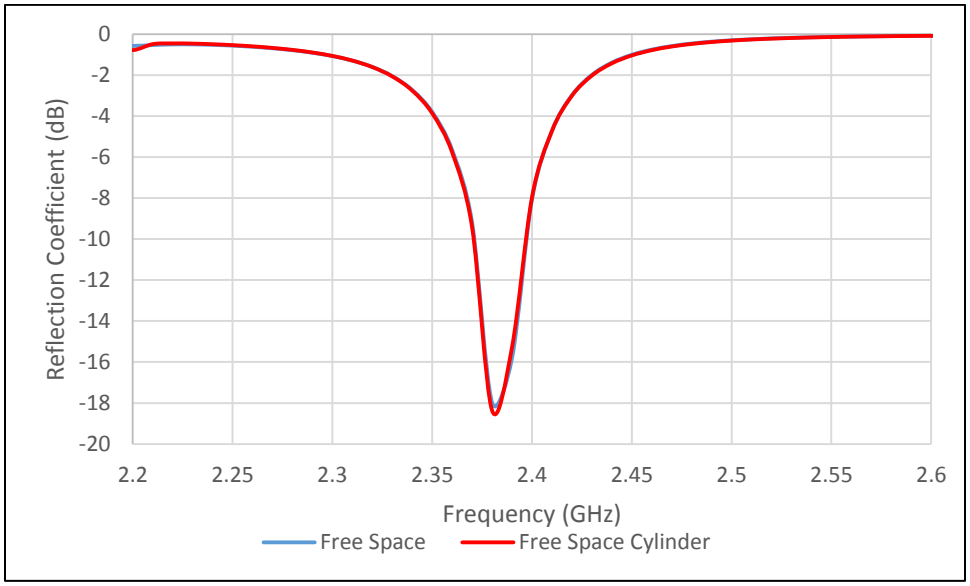

Figure 4.24: Reflection Coefficient Comparison between Antenna in the Free Space (Blue) and the Antenna on the Cylinder with the Parameters of the Free Space (Red)

A simulation giving to the cylinder the calculated properties of the human body at the operating frequency was performed. The calculated properties resulted in a dielectric constant of 37.31, conductivity of 1.33 S/m, and a los tangent of 0.24. Fig 4.24 shows a comparison in reflection coefficient for the original capacitively-fed folded slot antenna analyzed in section 4.1. For this configuration, the effect of the human body produced a reflection coefficient with 10 dB less than the free space conditions, at the same resonant frequency of 2.37 GHz.

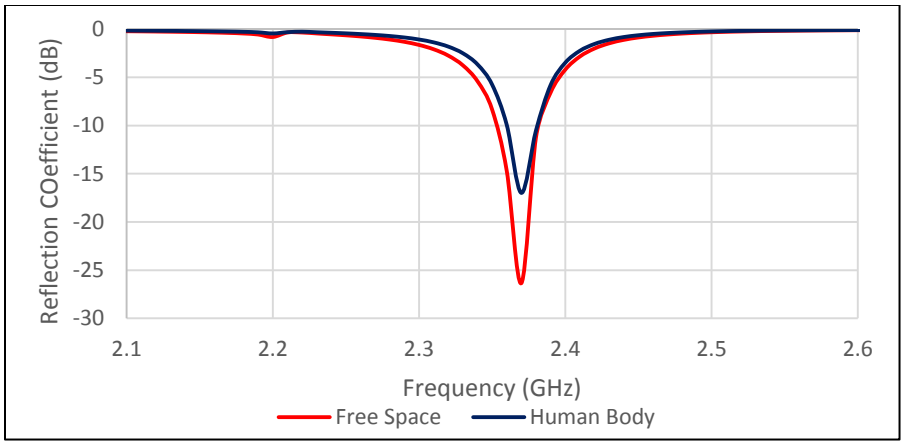

Figure 4.25 Reflection Coefficient Comparison between the Free Space Condition (red) and the calculates human body properties (blue) for the original capacitively-fed configuration

The simulation was conducted with the forearm in two different positions (slot along the forearm and slot across the forearm). In terms of reflection coefficient, the result shows a central frequency of 2.37 GHz and a magnitude of 2 dB bigger for the position 2 (slot across the forearm) as shown in Fig 4.25. In terms of the radiation pattern the position 2 has a front to back ratio of 3 dB better than the position 2 has less than one dB less gain. Fig 4.26 shows the comparison in radiation pattern between the two positions.

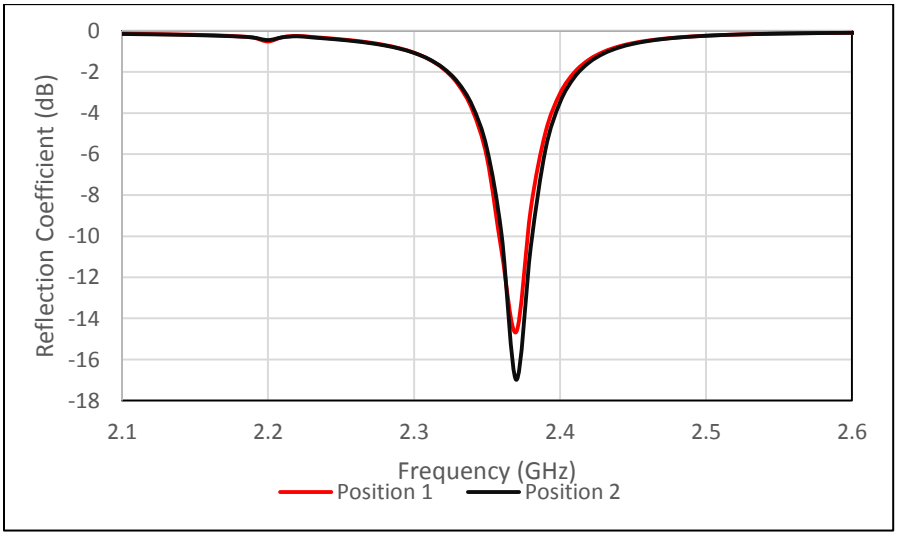

Figure 4.26: Reflection Coefficient Comparison between the Cylinder in Position 1 (red) and Position 2 (black)

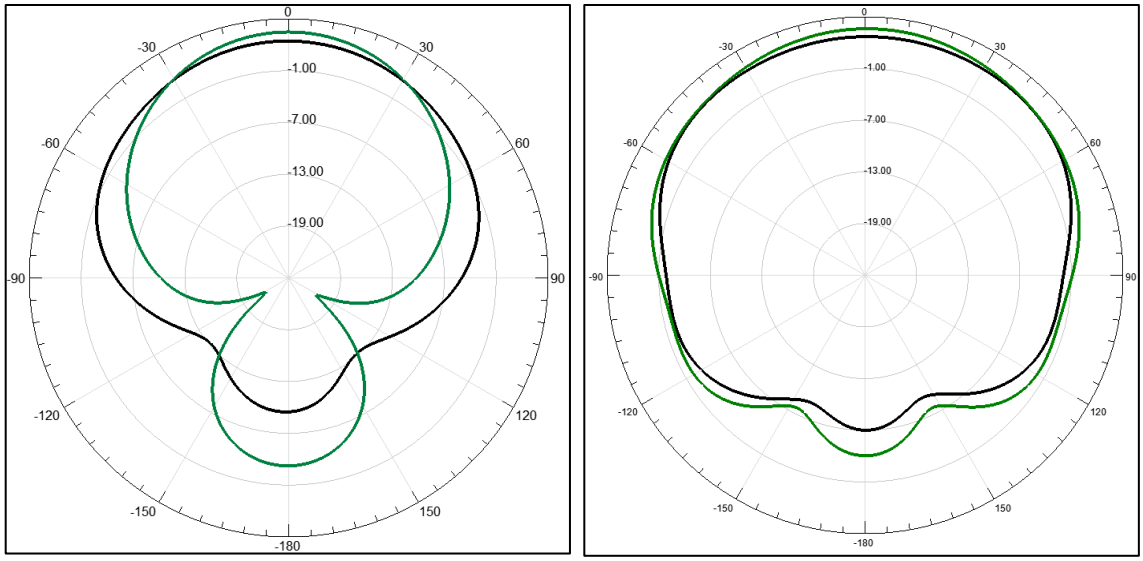

(a) (b)

Figure 4.27: Simulated Radiation Pattern Comparison between the Cylinder in the Position 1 (green) and Position 2 (black), in H-Plane (a) and E-Plane (b)

As a final step with the human tissue model, a comparison between this model with a five layer model was performed. The results was the same in both; radiation pattern and reflection coefficient. This can be explained because the calculated properties of the human body are very similar to the properties of the skin, which is the first layer of the multi-layer model. Fig. 4.27 shows the comparison between models in reflection coefficient, and Fig. 4.28 shows the comparison in the radiation pattern.

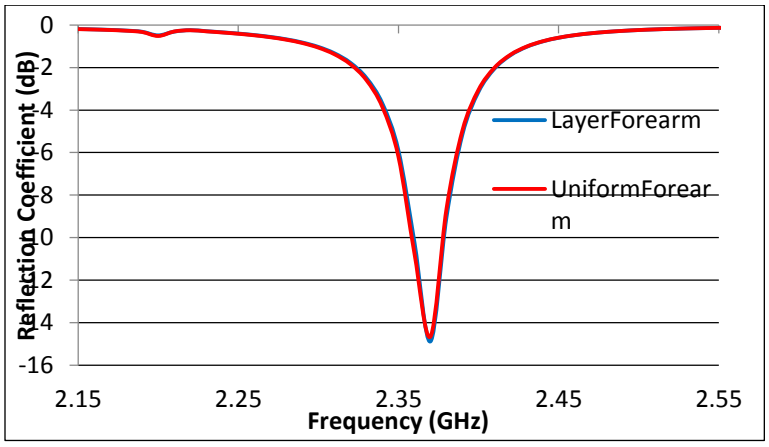

Figure 4.28 Reflection Coefficient Comparison between the Cylinder as a Uniform Layer (red) and Five Layer (blue)

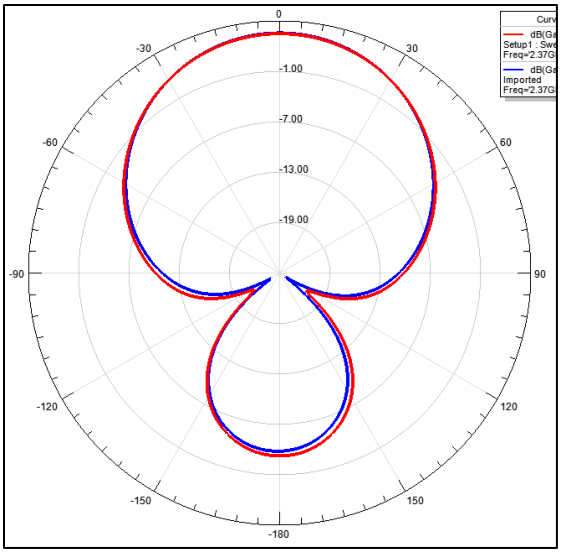

Figure 4.29 Radiation Pattern Comparison between the Cylinder as a Uniform Layer (red) and Five Layer (blue)

All of the antennas were simulated using the human body model. Based on the previous comparisons, position 2 was selected for all of the simulations. Figs. 4.29, 4.30 and 4.31 shows the results in terms of reflection coefficient and radiation pattern for the different antenna configurations.

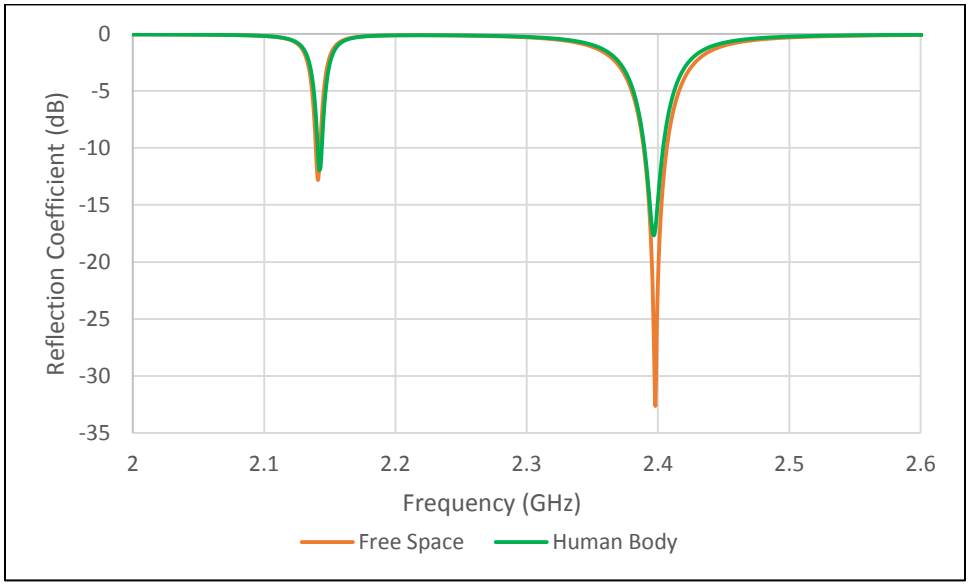

Figure 4.30: Free Space Properties (orange) vs Human Body Properties (green) comparison in S11 for the Modified Capacitively-Fed Folded Slot Antenna with a Ground Plane of 40 mm by 40 mm

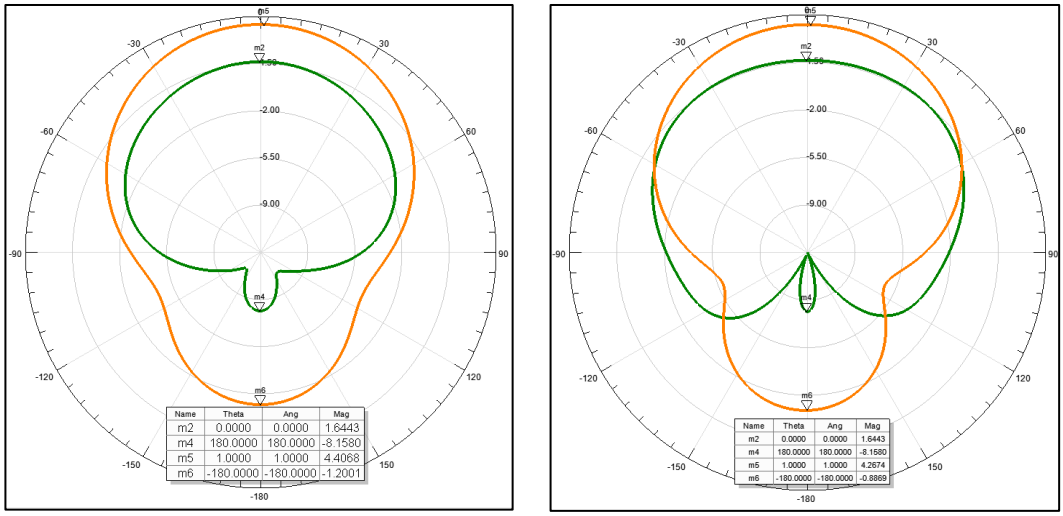

Figure 4.31: Free Space Properties (orange) vs Human Body Properties (green) comparison in Rad Pattern, in H-Plane (a) and E-Plane (b), for the Modified Capacitively-Fed Folded Slot Antenna with a Ground Plane of 40 mm by 40 mm

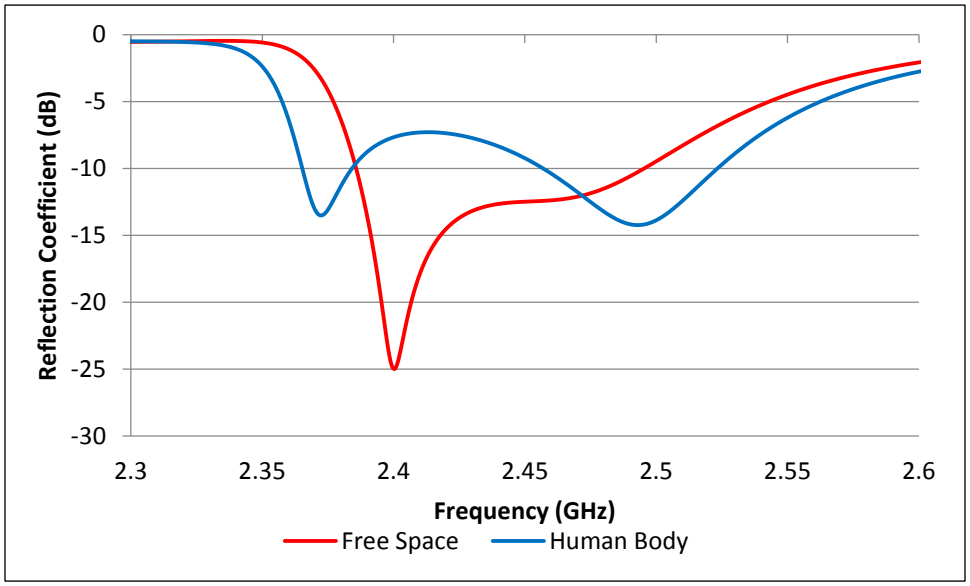

Figure 4.32: Free Space (red) vs Human Body (blue) Comparison in S11 for the Parasitic Patch Configuration

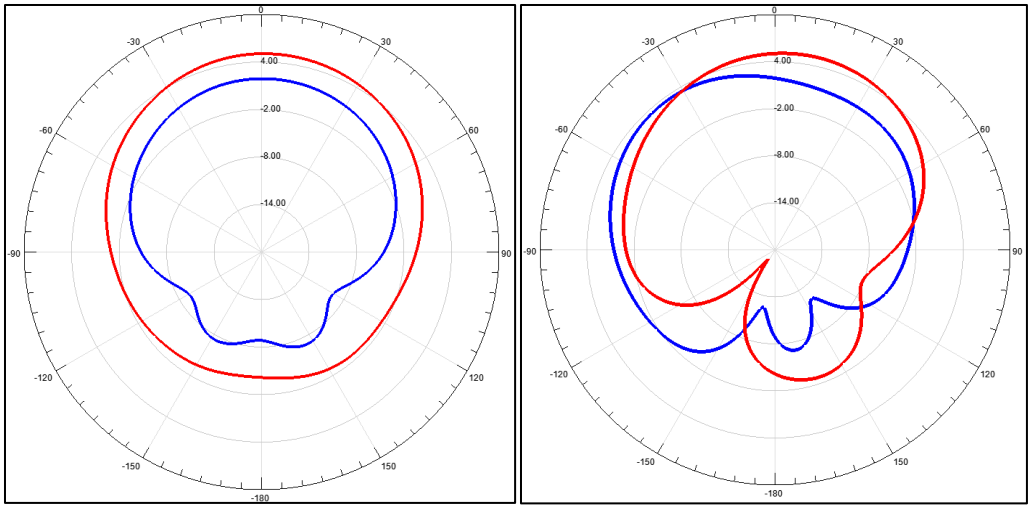

(a) (b)

Figure 4.33: Radiation Pattern in, H-Plane (a) and E-Plane (b), for Free Space Conditions (Red) and Human Body Condition (Blue)

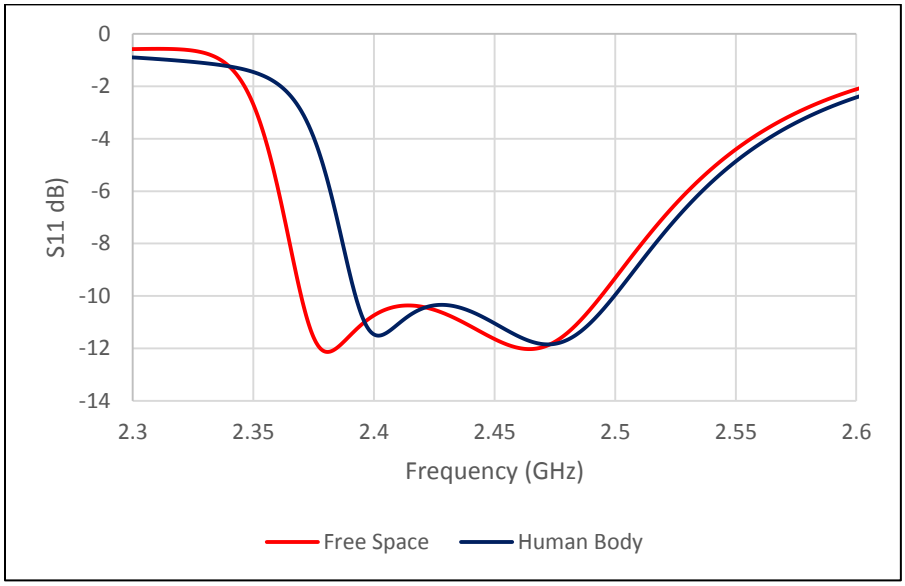

Figure 4.34: Free Space (red) vs Human Body (blue) Comparison in S11 for the Parasitic Patch Configuration After Modification to Improve Matching.

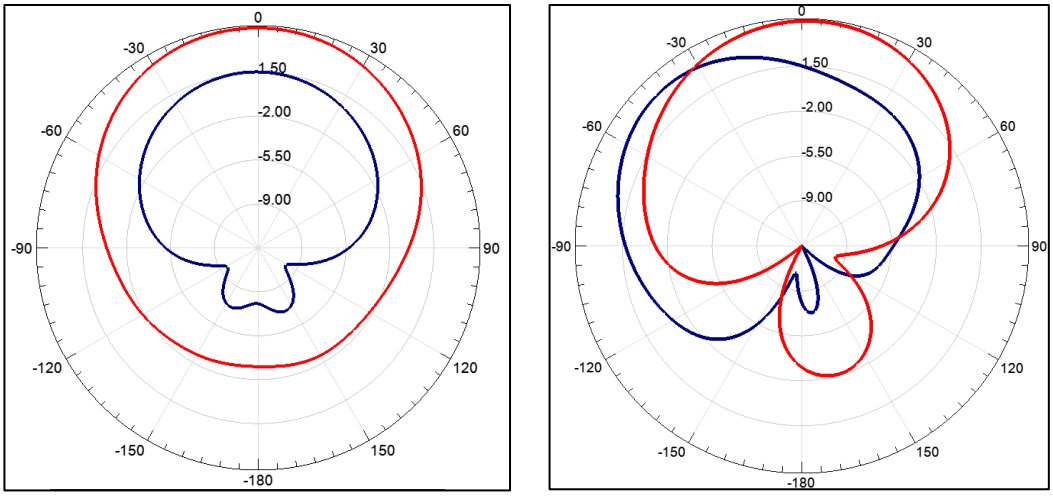

(a) (b)

Figure 4.35: Free Space (red) vs Human Body (blue) Comparison in Radiation Pattern in, H-Plane (a) and E-Plane (b), for the Parasitic Patch Configuration After Modification to Improve Matching.

The results presented in this chapter shown that the parasitic patch antenna works very well for the BCWC application, due to its behavior in bandwidth and gain. For the capacitively-fed antenna it works very well only in the radiation pattern and with a bandwidth comparable with previous works in slot antennas.

CHAPTER 5
CONCLUSION AND SUGGESTION FOR FUTURE WORK

Two new configurations; a cavity backed capacitively-fed folded slot antenna and a rectangular patch antenna, were disclosed in this thesis. Both configurations were modified to achieve the requirements for the body centric wireless communication application. The cavity-backed capacitevely-fed folded slot antenna was characterized, and the effects of its physical dimensions on the radiation pattern and input impedance were analyzed to better understand its performance. Once characterized, the antenna was modified by a change in the implementation of the cavity, due to an effect observed in the resonance of the antenna, and miniaturized by the loading slots technique. This configuration reduced the slot length from of 36 mm to 16 mm, maintaining a bandwidth and gain comparable with previous work in slot antennas.

The rectangular patch antenna was modified to reduce its size by making it a quarter-wave structure. The loading slot technique was also employed in this configuration and the size was reduced from 25 mm by 25 mm to 10.5 mm by 25 mm, also having a good performance in impedance and radiation pattern. A modification was made it to this configuration adding a parasitic patch, and a substrate change, to achieve the desired bandwidth. With these modifications the required bandwidth was achieved, and a good radiation performance was obtained through the frequency band. With the modifications the antenna results in a ground plane of 45 mm by 45 mm and the patch dimensions are 40 mm with and 26.68 mm of length.

A simple model of the human body was also proposed and developed in this thesis. The model was developed as a uniform cylinder with its electromagnetic properties calculated as a weighted average for the human tissues at the operating frequency. The calculations results in a

dielectric constant of 37.31, conductivity of 1.33 Siemens per meters, and a loss tangent of 0.24. The simulations of the antennas on the human tissue model show that the body does not affect the antenna performance in operating frequency. However a change in magnitude of the impedance was observed. Another effect observed placing the antennas on the human body was that the radiation pattern shows an improvement in the front to back ratio due to the energy absorbed by the body. This can be observed in the electric field distribution. This computational model was an excellent tool requiring much less computational time than software simulating the complete human body.

5.1 Suggestion for Future Work

This work presented a fully functional antenna for BCWC at the ISM band. The requirements were achieved with the parasitic patch configuration. This configuration could be improved in the future by making it smaller, by making the loading slots larger, or add more of them. In terms of the modified capacitively-fed folded slot antenna, the only goal achieved was the unidirectional pattern with a 40 mm by 40 mm ground plane. In the future a characterization to know what of the dimension affects the bandwidth is recommended. With the characterization, other techniques could be employed. For the human tissue analysis, other considerations such the shape and size of the model and additional layer that simulates clothing is also recommended. Future work also should include a fabrication of materials with the calculated electromagnetic properties, and test it with the antennas.

Appendix

Table A.1: Design Matrix for the Full Factorial Employed

RUN #	Lg	Sg	G	La	W3	W2	W1
0000000	6.12	0.18	0.18	32.22	0.18	1.8	0.36
0000001	6.12	0.18	0.18	32.22	0.18	1.8	0.44
0000010	6.12	0.18	0.18	32.22	0.18	2.2	0.36
0000011	6.12	0.18	0.18	32.22	0.18	2.2	0.44
0000100	6.12	0.18	0.18	32.22	0.22	1.8	0.36
0000101	6.12	0.18	0.18	32.22	0.22	1.8	0.44
0000110	6.12	0.18	0.18	32.22	0.22	2.2	0.36
0000111	6.12	0.18	0.18	32.22	0.22	2.2	0.44
0001000	6.12	0.18	0.18	39.38	0.18	1.8	0.36
0001001	6.12	0.18	0.18	39.38	0.18	1.8	0.44
0001010	6.12	0.18	0.18	39.38	0.18	2.2	0.36
0001011	6.12	0.18	0.18	39.38	0.18	2.2	0.44
0001100	6.12	0.18	0.18	39.38	0.22	1.8	0.36
0001101	6.12	0.18	0.18	39.38	0.22	1.8	0.44
0001110	6.12	0.18	0.18	39.38	0.22	2.2	0.36
0001111	6.12	0.18	0.18	39.38	0.22	2.2	0.44
0010000	6.12	0.18	0.22	32.22	0.18	1.8	0.36
0010001	6.12	0.18	0.22	32.22	0.18	1.8	0.44
0010010	6.12	0.18	0.22	32.22	0.18	2.2	0.36
0010011	6.12	0.18	0.22	32.22	0.18	2.2	0.44
0010100	6.12	0.18	0.22	32.22	0.22	1.8	0.36
0010101	6.12	0.18	0.22	32.22	0.22	1.8	0.44
0010110	6.12	0.18	0.22	32.22	0.22	2.2	0.36
0010111	6.12	0.18	0.22	32.22	0.22	2.2	0.44
0011000	6.12	0.18	0.22	39.38	0.18	1.8	0.36
0011001	6.12	0.18	0.22	39.38	0.18	1.8	0.44
0011010	6.12	0.18	0.22	39.38	0.18	2.2	0.36
0011011	6.12	0.18	0.22	39.38	0.18	2.2	0.44
0011100	6.12	0.18	0.22	39.38	0.22	1.8	0.36
0011101	6.12	0.18	0.22	39.38	0.22	1.8	0.44
0011110	6.12	0.18	0.22	39.38	0.22	2.2	0.36
0011111	6.12	0.18	0.22	39.38	0.22	2.2	0.44
0100000	6.12	0.22	0.18	32.22	0.18	1.8	0.36
0100001	6.12	0.22	0.18	32.22	0.18	1.8	0.44
0100010	6.12	0.22	0.18	32.22	0.18	2.2	0.36
0100011	6.12	0.22	0.18	32.22	0.18	2.2	0.44
0100100	6.12	0.22	0.18	32.22	0.22	1.8	0.36
0100101	6.12	0.22	0.18	32.22	0.22	1.8	0.44
0100110	6.12	0.22	0.18	32.22	0.22	2.2	0.36

Run#	Lg	Sg	G	La	W3	W2	W1
0100111	6.12	0.22	0.18	32.22	0.22	2.2	0.44
0101000	6.12	0.22	0.18	39.38	0.18	1.8	0.36
0101001	6.12	0.22	0.18	39.38	0.18	1.8	0.44
0101010	6.12	0.22	0.18	39.38	0.18	2.2	0.36
0101011	6.12	0.22	0.18	39.38	0.18	2.2	0.44
0101100	6.12	0.22	0.18	39.38	0.22	1.8	0.36
0101101	6.12	0.22	0.18	39.38	0.22	1.8	0.44
0101110	6.12	0.22	0.18	39.38	0.22	2.2	0.36
0101111	6.12	0.22	0.18	39.38	0.22	2.2	0.44
0110000	6.12	0.22	0.22	32.22	0.18	1.8	0.36
0110001	6.12	0.22	0.22	32.22	0.18	1.8	0.44
0110010	6.12	0.22	0.22	32.22	0.18	2.2	0.36
0110011	6.12	0.22	0.22	32.22	0.18	2.2	0.44
0110100	6.12	0.22	0.22	32.22	0.22	1.8	0.36
0110101	6.12	0.22	0.22	32.22	0.22	1.8	0.44
0110110	6.12	0.22	0.22	32.22	0.22	2.2	0.36
0110111	6.12	0.22	0.22	32.22	0.22	2.2	0.44
0111000	6.12	0.22	0.22	39.38	0.18	1.8	0.36
0111001	6.12	0.22	0.22	39.38	0.18	1.8	0.44
0111010	6.12	0.22	0.22	39.38	0.18	2.2	0.36
0111011	6.12	0.22	0.22	39.38	0.18	2.2	0.44
0111100	6.12	0.22	0.22	39.38	0.22	1.8	0.36
0111101	6.12	0.22	0.22	39.38	0.22	1.8	0.44
0111110	6.12	0.22	0.22	39.38	0.22	2.2	0.36
0111111	6.12	0.22	0.22	39.38	0.22	2.2	0.44
1000000	7.48	0.18	0.18	32.22	0.18	1.8	0.36
1000001	7.48	0.18	0.18	32.22	0.18	1.8	0.44
1000010	7.48	0.18	0.18	32.22	0.18	2.2	0.36
1000011	7.48	0.18	0.18	32.22	0.18	2.2	0.44
1000100	7.48	0.18	0.18	32.22	0.22	1.8	0.36
1000101	7.48	0.18	0.18	32.22	0.22	1.8	0.44
1000110	7.48	0.18	0.18	32.22	0.22	2.2	0.36
1000111	7.48	0.18	0.18	32.22	0.22	2.2	0.44
1001000	7.48	0.18	0.18	39.38	0.18	1.8	0.36
1001001	7.48	0.18	0.18	39.38	0.18	1.8	0.44
1001010	7.48	0.18	0.18	39.38	0.18	2.2	0.36
1001011	7.48	0.18	0.18	39.38	0.18	2.2	0.44
1001100	7.48	0.18	0.18	39.38	0.22	1.8	0.36
1001101	7.48	0.18	0.18	39.38	0.22	1.8	0.44
1001110	7.48	0.18	0.18	39.38	0.22	2.2	0.36

Run#	Lg	Sg	G	La	W3	W2	W1
1001111	7.48	0.18	0.18	39.38	0.22	2.2	0.44
1010000	7.48	0.18	0.22	32.22	0.18	1.8	0.36
1010001	7.48	0.18	0.22	32.22	0.18	1.8	0.44
1010010	7.48	0.18	0.22	32.22	0.18	2.2	0.36
1010011	7.48	0.18	0.22	32.22	0.18	2.2	0.44
1010100	7.48	0.18	0.22	32.22	0.22	1.8	0.36
1010101	7.48	0.18	0.22	32.22	0.22	1.8	0.44
1010110	7.48	0.18	0.22	32.22	0.22	2.2	0.36
1010111	7.48	0.18	0.22	32.22	0.22	2.2	0.44
1011000	7.48	0.18	0.22	39.38	0.18	1.8	0.36
1011001	7.48	0.18	0.22	39.38	0.18	1.8	0.44
1011010	7.48	0.18	0.22	39.38	0.18	2.2	0.36
1011011	7.48	0.18	0.22	39.38	0.18	2.2	0.44
1011100	7.48	0.18	0.22	39.38	0.22	1.8	0.36
1011101	7.48	0.18	0.22	39.38	0.22	1.8	0.44
1011110	7.48	0.18	0.22	39.38	0.22	2.2	0.36
1011111	7.48	0.18	0.22	39.38	0.22	2.2	0.44
1100000	7.48	0.22	0.18	32.22	0.18	1.8	0.36
1100001	7.48	0.22	0.18	32.22	0.18	1.8	0.44
1100010	7.48	0.22	0.18	32.22	0.18	2.2	0.36
1100011	7.48	0.22	0.18	32.22	0.18	2.2	0.44
1100100	7.48	0.22	0.18	32.22	0.22	1.8	0.36
1100101	7.48	0.22	0.18	32.22	0.22	1.8	0.44
1100110	7.48	0.22	0.18	32.22	0.22	2.2	0.36
1100111	7.48	0.22	0.18	32.22	0.22	2.2	0.44
1101000	7.48	0.22	0.18	39.38	0.18	1.8	0.36
1101001	7.48	0.22	0.18	39.38	0.18	1.8	0.44
1101010	7.48	0.22	0.18	39.38	0.18	2.2	0.36
1101011	7.48	0.22	0.18	39.38	0.18	2.2	0.44
1101100	7.48	0.22	0.18	39.38	0.22	1.8	0.36
1101101	7.48	0.22	0.18	39.38	0.22	1.8	0.44
1101110	7.48	0.22	0.18	39.38	0.22	2.2	0.36
1101111	7.48	0.22	0.18	39.38	0.22	2.2	0.44
1110000	7.48	0.22	0.22	32.22	0.18	1.8	0.36
1110001	7.48	0.22	0.22	32.22	0.18	1.8	0.44
1110010	7.48	0.22	0.22	32.22	0.18	2.2	0.36
1110011	7.48	0.22	0.22	32.22	0.18	2.2	0.44
1110100	7.48	0.22	0.22	32.22	0.22	1.8	0.36
1110101	7.48	0.22	0.22	32.22	0.22	1.8	0.44
1110110	7.48	0.22	0.22	32.22	0.22	2.2	0.36

Run#	Lg	Sg	G	La	W3	W2	W1
1110111	7.48	0.22	0.22	32.22	0.22	2.2	0.44
1111000	7.48	0.22	0.22	39.38	0.18	1.8	0.36
1111001	7.48	0.22	0.22	39.38	0.18	1.8	0.44
1111010	7.48	0.22	0.22	39.38	0.18	2.2	0.36
1111011	7.48	0.22	0.22	39.38	0.18	2.2	0.44
1111100	7.48	0.22	0.22	39.38	0.22	1.8	0.36
1111101	7.48	0.22	0.22	39.38	0.22	1.8	0.44
1111110	7.48	0.22	0.22	39.38	0.22	2.2	0.36
1111111	7.48	0.22	0.22	39.38	0.22	2.2	0.44

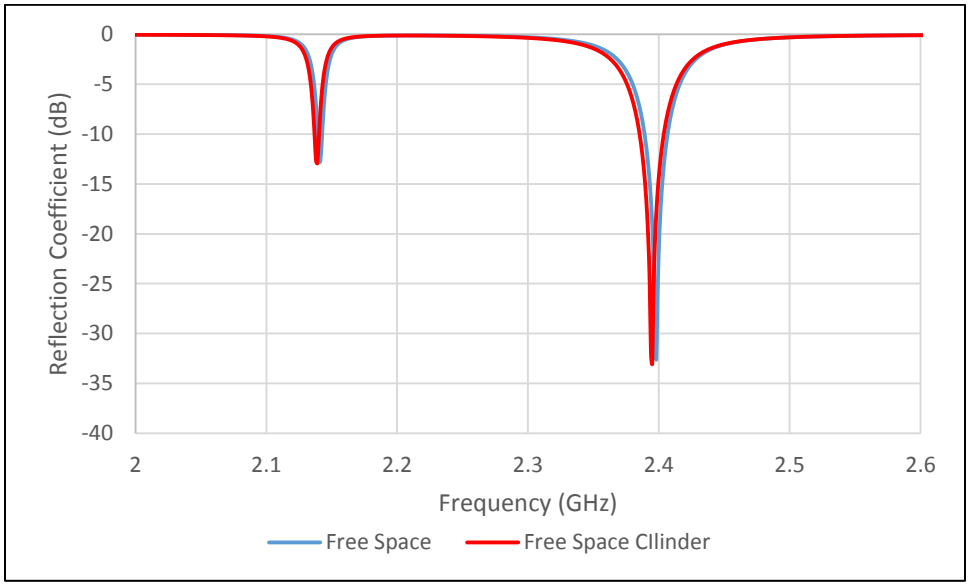

Figure A.1: Free Space Cylinder (Red) vs Free Space (blue) Comparison in S11 for the Modified Capacitively-fed folded Slot Antenna in a ground Plane of 40 mm by 40 mm

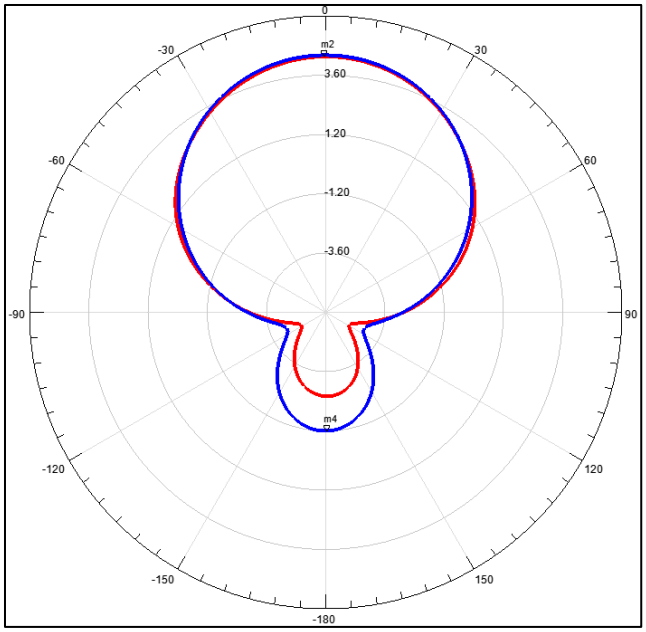

Figure A.2: Free Space Cylinder (Red) vs Free Space (blue) Comparison in in Gain for the Modified Capacitively-fed folded Slot Antenna in a Ground Plane of 40 mm by 40 mm

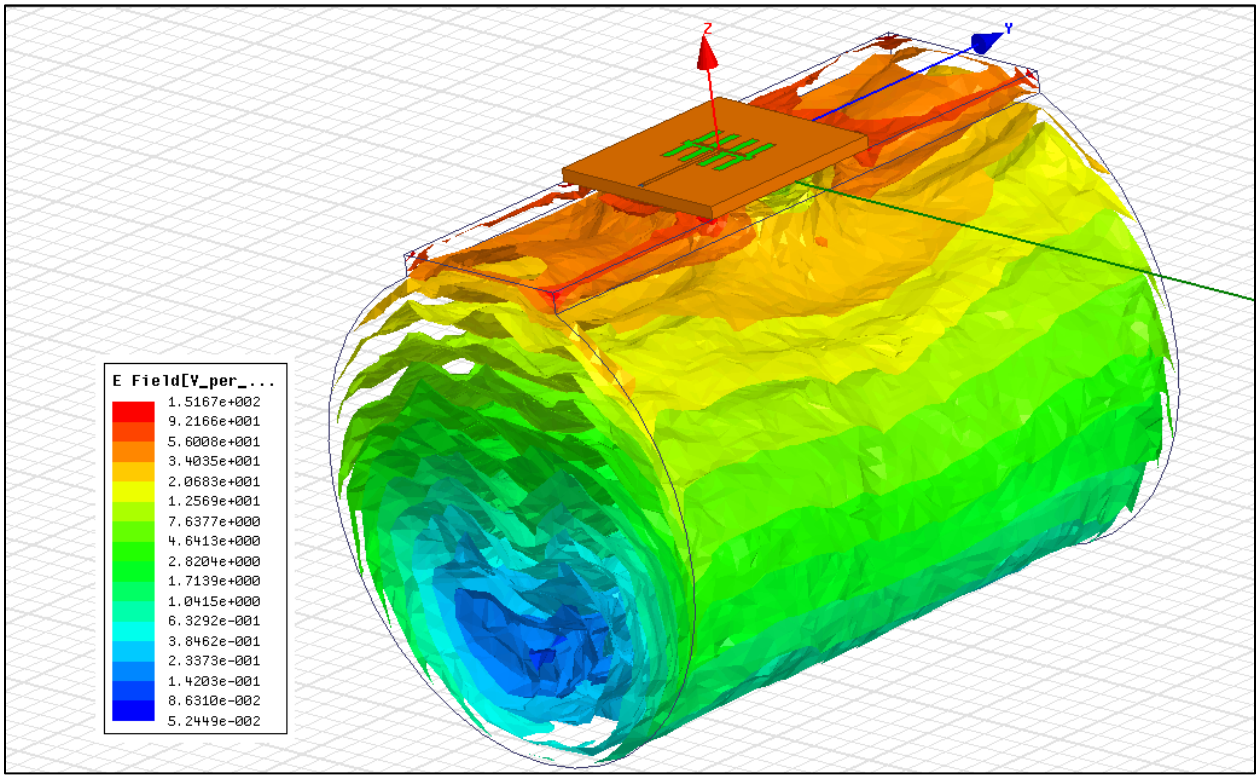

Figure A.3 Electric Field Distribution in the Human Body for the Modified Capacitively Fed Folded Slot Antenna

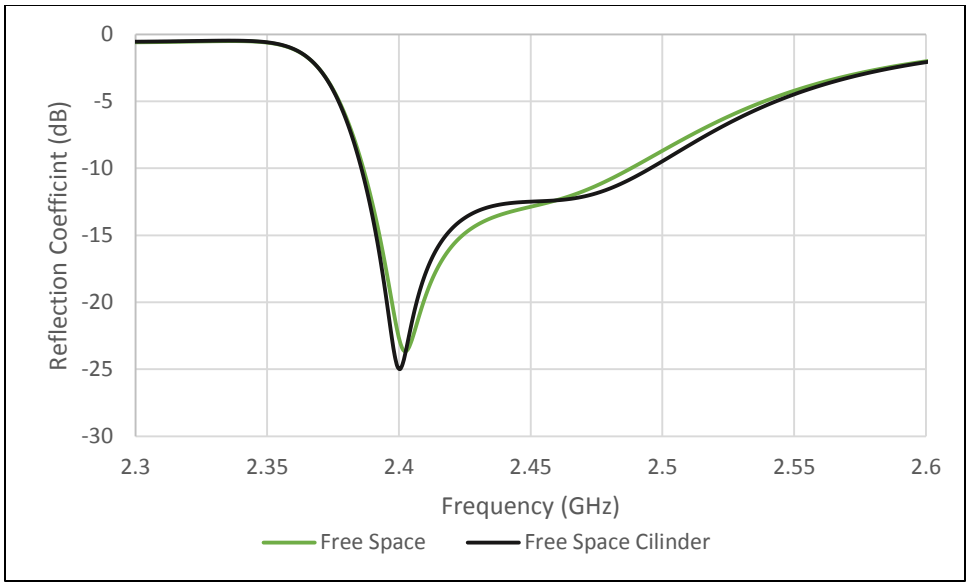

Figure A.4: Free Space vs Free Space Cylinder Comparison in S11 for the Modified Capacitively-fed folded Slot Antenna

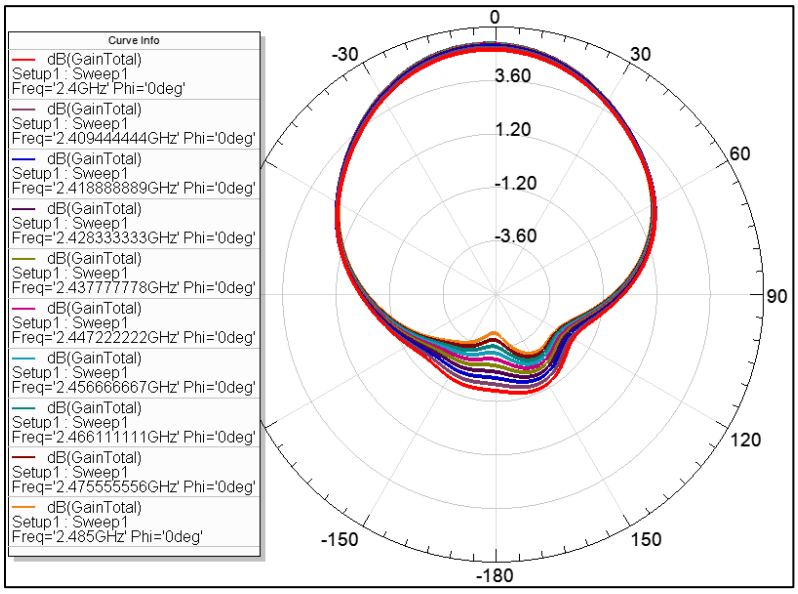

Figure A.5 Radiation Pattern Under Free Space Condition for the Parasitic Patch

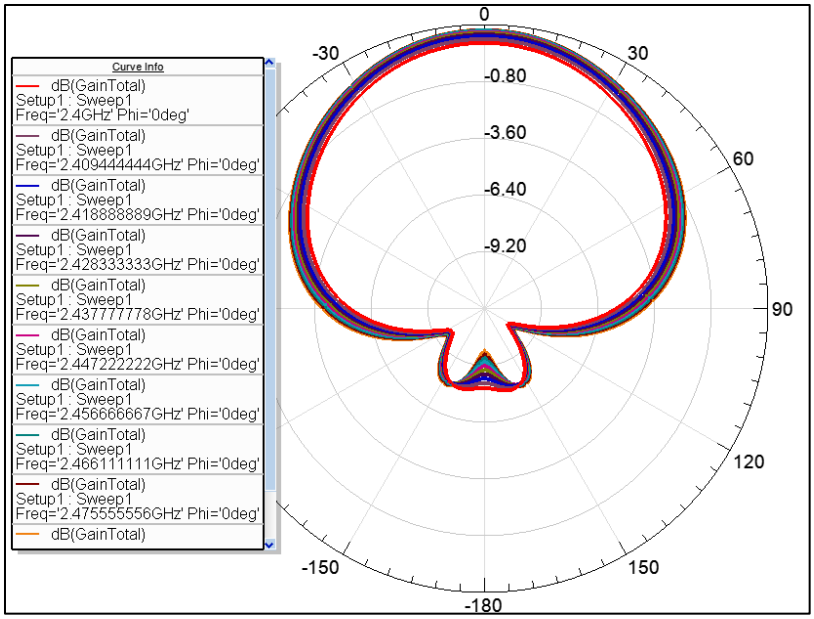

Figure A. 6 Radiation Pattern Under Human Body Condition for the Parasitic Patch

REFERENCE LIST

[1] A. Pellegrini, A. Brizzi, L. Zhang, K. Ali, Y. Hao, X. Wu, C. C. Constantinou, Y. Nechayev, P. S. Hall, N. Chahat, M. Zhadobov, and R. Sauleau, "Antennas and propagation for body-centric wireless communications at millimeter-wave frequencies: A review," *IEEE Antennas and Propagation Magazine*, vol. 55. pp. 262–287, 2013

[2] Rius, R.M.; Talavera, G.; Carrabina, J., "Developing and study of wearable and flexible antennas for Body Area Networks working under extreme conditions," *Antenna Technology and Applied Electromagnetics (ANTEM), 2012 15th International Symposium on* , vol., no., pp.1,5, 25-28 June 2012

[3] Guangdong Liu; Degong Wang; Fulu Jin; Shuo Chang, "Compact broad dual-band antenna using a shorted patch with a thick air substrate for wireless body area network application," *Microwave, Antenna, Propagation, and EMC Technologies for Wireless Communications (MAPE), 2011 IEEE 4th International Symposium on* , vol., no., pp.18,21, 1-3 Nov. 2011

[4] B. Buxton, "*Wearing a Wire: Simulation helps to optimize body-worn wireless devices for an emerging class of applications*", Electronics Synapse Product Development in Seattle, U.S.A., ANSYS Advantage Magazine Journal, Vol. 6, No. 2, 2012.

[5] P.S Hall and Y.Hao, "*Antennas and Propagation for Body Centric Wireless" Communications, Norwood, MA,Artech House, 2006*

[6] Ramli, N.H.; Ahyat, E. N.; Kamarudin, M.R.; Samsuri, N. A; Rahim, M. K A; Khamis, N.H., "Design & optimization of a compact ring monopole antenna for wireless implantable body area network (WiBAN) applications," *Microwave*

Conference Proceedings (APMC), 2011 Asia-Pacific , vol., no., pp.1602,1609, 5-8 Dec. 2011

[7] Chia-Hsien Lin; Saito, K.; Takahashi, M.; Ito, K., "A Compact Planar Inverted-F Antenna for 2.45 GHz On-Body Communications," *Antennas and Propagation, IEEE Transactions on* , vol.60, no.9, pp.4422,4426, Sept. 2012

[8] Chandran, A.R.; Conway, G.A.; Scanlon, W.G., "Pattern switching compact patch antenna for on-body and off-body communications at 2.45 GHz," *Antennas and Propagation, 2009. EuCAP 2009. 3rd European Conference on* , vol., no., pp.2055,2057, 23-27 March 2009

[9] Raman, S.; Graham, B.; Crossan, S.M.; Timmons, N.; Morrison, J.; Shameena, V.A.; Pezholil, M., "Microstrip fed ground modified compact antenna with reconfigurable radiation pattern for BANs," *Antennas and Propagation Conference (LAPC), 2012 Loughborough* , vol., no., pp.1,4, 12-13 Nov. 2012

[10] J.Volakis, et.al "Small Antennas Miniaturization Techniques & Applications", Mc Graw Hill, 2010

[11] Van Caekenberghe, K.; Behdad, N.; Brakora, K.M.; Sarabandi, K., "A 2.45-GHz Electrically Small Slot Antenna," *Antennas and Wireless Propagation Letters, IEEE* , vol.7, no., pp.346,348, 2008

[12] R.Garg, et.al "Microstrip Antenna Design Handbook", Artech House, MA, 2001.

[13] Córdoba-Erazo, M.F.; Rodriguez-Solis, R.A, "Cavity-backed folded-slot antenna," *Antennas and Propagation Society International Symposium (APSURSI), 2010 IEEE*, vol., no., pp.1,4, 11-17 July 2010

[14] D. C Montgomery, "*Design of Experiments"* 8th edition New York: Wiley 2000

[15] Cordoba Erazo, Maria F, "*Characterization of Cavity-Backed Folded Slot Antennas",* University of Puerto Rico, Mayaguez, ProQuest, 2009

[16] Valentin, E.; Rodriguez-Solis, R.A., "Characterization of a cavity-backed capacitively-fed folded slot antenna using DOE techniques," *Antennas and Propagation Society International Symposium (APSURSI), 2014 IEEE* , vol., no., pp.1499,1500, 6-11 July 2014

[17] Lopez-Rivera, Nestor David, "*Characterization and Modeling of Folded Slot Antenna",* University of Puerto Rico, Mayaguez, ProQuest, 2003

[18] Del Rio, David, *"Characterization of Log Peridic Folded Slot Antenna Array"*, University of Puerto Rico, Mayaguez, 2005

[19] D. Pozar, *"Microwave Engineering", 4th edition, Wiley 2012*

[20] C.Balanis,*"Advance Electromagnetics Engineering", 2nd edition, New York Wiley,2012*

[21] M. Sadiku, "*Elements of Electromagnetics", 6th edition, New York, Oxford, 2015*

[22] Lopez-Rivera, N, Rodriguez-Solis R.A., "*Impoedance Matching Technique for Microwave Folded Slot Antenna"*, Antennas and Propagation Society Symposium, 2002.

[23] Lopez-Rivera, N.D.; Rodriguez-Solis, R.A., "Input impedance and resonant frequency characterization for folded slot antennas through DOE techniques," *Antennas and Propagation Society International Symposium, 2003. IEEE* , vol.2, no., pp.545,548 vol.2, 22-27 June 2003

[24] C Balanis, *"Antenna Theory and Analysis and Design"*, 3rd edition, New York, Wiley, 2005

[25] Kumar G, K.P. Ray, *"Broadband Microstrip Antennas",* Norwood, Artech House, 2003

[26] Ito, K.; Haga, N.; Takahashi, M.; Saito, K., "Evaluations of Body-Centric Wireless Communication Channels in a Range From 3 MHz to 3 GHz," *Proceedings of the IEEE* , vol.100, no.7, pp.2356,2363, July 2012